Received: 28 April 2021 | Accepted: 16 August 2021

DOI: 10.1002/jpln.202100138

REGULAR ARTICLE

Spatial 3D mapping of forest soil carbon stocks in Hesse, Germany

Felix Heitkamp | **Bernd Ahrends** | **Jan Evers** | **Henning Meesenburg**

Environmental Control, Northwest German Forest Research Institute, Grätzelstraße 2, Göttingen, Germany

Correspondence
Dr. Felix Heitkamp, Environmental Control, Northwest German Forest Research Institute, Grätzelstraße 2, 37079 Göttingen, Germany.
Email: felix.heitkamp@nw-fva.de

Funding information
Hessisches Ministerium für Umwelt, Klimaschutz, Landwirtschaft und Verbraucherschutz, Grant/Award Numbers: Integrierter Klimaschutzplan Hessen 2025, L–12, LF–06

Abstract

Background: Forest soils are an important reservoir of organic carbon (OC) and a potential source or sink for atmospheric CO_2. Prediction of OC stock changes under ongoing climatic and management changes requires a spatial explicit base. Knowledge of the vertical distribution of OC stocks is very important, since varying soil layers may be affected differently by environmental change.

Aim: Three-dimensional regionalization of OC stocks of the forest floor (FFC) and 5 cm depth increments of the mineral soil (SOC) of Hesse, Germany.

Methods: Datasets of the second National Forest Soil Inventory (NFSI II) were used for parametrization of hierarchical generalized additive models (hGAM). Validation was performed by a 10 times repeated 10-fold cross-validation, and spatial model uncertainty was assessed.

Results: Depth-dependent validation indicated that model performance was best between 15 and 60 cm (amount of variance explained ≈ 0.5). All covariates showed plausible partial effects. FFC stocks were predicted to be highest under coniferous forest with a high influence of N deposition. Climate and potential cation exchange capacity affected SOC stocks markedly, whereas soil class and parent material were most important for the depth distribution. Overall, average predicted OC stocks were between 78.0 and 92.5 t ha^{-1}, amounting to 67.6 to 80.1 Mt for all forest soils of Hesse. Between 16% and 24% were stored in the forest floor. Sixty-eight percent to 69% of predicted SOC stocks were stored in the upper 30 cm. Model uncertainty was highest at locations with high elevation or ground water influence.

Conclusions: This work provides the first spatial explicit database for OC stocks of forest soils in Hesse at an intermediate scale. Stocks can be assessed flexibly for varying depth from the forest floor down to 100 cm. Uncertainty analysis informs about locations, where the model results have to be handled with care.

KEYWORDS
depth distribution, hierarchical generalized additive model (hGAM), National Forest Soil Inventory, regionalization, SCORPAN, uncertainty

1 | INTRODUCTION

One of the manifold services of forest ecosystems is carbon (C) sequestration. Globally, forests store about 80% of terrestrial aboveground biomass and 70% of soil organic carbon (SOC; Jandl et al., 2007). de Vos et al. (2015) estimated the total forest SOC stock for 22 EU countries to 21 Gt down to 100 cm, and an additional 3.5 to 4 Gt C in forest floors (FFC). At least one-third of SOC was stored below the topsoil (30 cm depth). Especially forest floor and topsoil organic carbon is sensitive to environmental changes, such as climate and management (Jandl et al., 2007). However, the trajectory of changing organic carbon (OC) stocks in forest soils over time strongly depends on specific site conditions, dynamic equilibrium state, the capacity of soils to stabilize C, or initial forest stand and tree species (Angst et al., 2019; Mayer et al., 2020; Soucémarianadin et al., 2018).

There is a great effort in monitoring of FFC and SOC stocks through space and time, such as the International Co-operative Programme on Assessment and Monitoring of Air Pollution Effects on Forests (ICP Forests Level II) or extensive national forest soil inventories (NFSI; de Vos et al., 2015; Fleck et al., 2016; Wellbrock et al., 2019). The grid-based sampling approach in extensive monitoring gives by design representative values for larger areas (Webster and Oliver, 2007). Repeated sampling also documents changes in C stocks over time, although small-scale heterogeneity of soil properties introduces considerable uncertainty (Kravchenko and Robertson, 2011; Meiwes et al., 2009; Schrumpf et al., 2011). Moreover, changes can be interpreted in retrospective, but projections based on climate and management scenarios are needed for sustainable planning in forestry (Albert et al., 2017). Spatially explicit information is a necessary prerequisite for sound decisions, but availability is scarce, especially regarding OC stocks at intermediate scales (Arrouays et al., 2020). This also holds true if the vertical distribution of OC across the soil profile is desired (Nauman and Duniway, 2019).

Mapping of soil properties generally bases on relationships between the variable of interest and environmental factors (Jenny, 1941; McBratney et al., 2003). These relationships are quantified by various (geo-)statistical models, such as machine learning, regression-like models, co-kriging, or combined approaches (Cianfrani et al., 2018). Often, total stocks or mean concentrations without information on vertical distribution of OC were predicted (*e.g.*, de Brogniez et al., 2015; Fleck et al., 2017; Heitkamp et al., 2020). Three-dimensional information of OC stocks, however, is important because environmental changes affect OC in varying depth differently. Data from the first and second NFSI in Germany demonstrated that FFC stocks declined in some regions, but this was more than compensated by increasing SOC stocks in the topsoil (Grüneberg et al., 2019). Therefore, dynamic modeling will benefit from knowledge of vertical OC distributions (Camino-Serrano et al., 2018; Ziche et al., 2019). There are two main approaches for modeling spatial explicit depth distributions. For the so-called 2.5D approach, OC contents or stocks are estimated separately for predefined depth increments. This has the advantage that model complexity is relatively low, but at the cost of multiple model setup and parametrization. Moreover, predictions for predefined depth increments may not be flexible enough for users' needs, disconnected models can produce discontinuous profiles, and uncertainty analysis across the profile is challenging (Hengl et al., 2014). In 3D models, either a depth function is predicted into space (Yang et al., 2016), or "depth" is directly incorporated as a covariate in the predictive model (Ma et al., 2021, and references therein). These approaches potentially circumvent some disadvantages of 2.5D modeling. However, using depth as a covariate was shown to increase uncertainty in data-driven approaches (Ma et al., 2021; Nauman and Duniway, 2019). Ma et al. (2021) therefore recommended to develop pedological knowledge-driven approaches.

The magnitude of soil SOC stocks depends on the complex interaction between temperature, moisture, soil properties (*e.g.*, texture, pH values), tree species, forest management, and litter quality (Burke et al., 1989; Carey et al., 2020; Lal, 2005). With climate change, however, not only temperatures and moisture will change in the future, but also the amount and quality of litterfall due to intentional or unintentional changes in tree species. The projected changes in soil water conditions could have significant impacts on forests growth, biogeochemical cycles, and biotic or abiotic risks, especially for the widespread Norway spruce stands (Panferov et al., 2009; Thiele et al., 2017). Thus, there is a need for adaptive management strategies including the introduction of alternative tree species and higher proportions of mixed instead of monospecific, often pure coniferous forest stands (Paul et al., 2019; Temperli et al., 2012). A first step to guide OC preserving management is the provision of spatial explicit information on the three-dimensional distribution of OC stocks.

Our objectives were to predict FFC and depth distribution of SOC stocks in forest soils by (1) parameterization of a parsimonious 3D model using data of the NFSI and pedological knowledge (Ma et al., 2019), and (2) quantify associated spatial uncertainty. The federal state of Hesse, Germany, was used as an exemplary region.

2 | MATERIALS AND METHODS

2.1 | Study area

The federal state of Hesse is situated in Central Germany. Climate is temperate-humid and mean annual temperature (MAT, 5.2 to 10.6°C) and precipitation (MAP, 537 to 1385 mm y^{-1}) in the period from 1971 to 2000 depend strongly on elevation (80 to 950 m above sea level). Forests cover 42% (8690 km^2) of Hesse. European beech (*Fagus sylvatica* L.) is the most frequent species (ca. 31%), followed by Norway spruce (ca. 22%; *Picea abies* [L.] H.KARST), oak (ca. 14%, *Quercus spp.* L.), and pine (ca. 10%, *Pinus spp.* L.; Hessisches Ministerium für Umwelt, Klimaschutz, Landwirtschaft und Verbraucherschutz, 2015). Mixed forest stands dominate (51%) while coniferous and broadleaved stands have similar proportions (27% and 22%, respectively; HVBG, 2018). Parent material of forest soils often (86%) contains variable

proportions of loess with solifluctive mixing with acidic, base poor, base rich, or carbonatic bedrock. Fluviatile substrates (6%), eolic sand (4%), and deep loess (4%) are less important, but still notable parent materials. Cambisols (63%), Stagnosols (12%), and Luvisols (12%) are the most widespread Reference Soil Groups, and Anthrosols (colluvial), Leptosols, and Gleysols each cover 3.5% to 4%. Histosols make up only 0.1% of the forest area. However, Gleysols and Stagnosols may contain histic horizons. More details can be found in Heitkamp et al. (2020).

2.2 | National Forest Soil Inventory

The second National Forest Soil Inventory (NFSI) took place between 2006 and 2008 along an 8 × 8 km grid. The number of sampling plots in Hesse (n = 139) was too low to fit complex statistical models. Therefore, NFSI plots of the neighboring federal states Lower Saxony and Saxony-Anhalt were added to the dataset (n = 380). The full dataset of the three federal states with similar environmental conditions was used for model parametrization and validation, while predictions were applied to the soil map polygons of Hesse. Each sampling plot was described regarding environmental conditions, such as tree species composition, topographical attributes, and, as far as possible, site history. A soil profile and 8 additional points (satellites) placed around the profile (r = 10 m) were characterized and sampled at every grid point. A mixed sample was created from the profile and the satellites. A very detailed description of the sampling layout, including a map with sampling points, is provided by Wellbrock et al. (2019). Sampling depth was at least down to bedrock or 90 cm. Sampling was stratified according to depth into the forest floor and intervals of 0–5, 5–10, 10–30, 30–60, and 60–90 cm. Sampling, sample preparation and analysis followed standardized procedures (Evers et al., 2019; Paar et al., 2016; Wellbrock et al., 2019). Briefly, all samples were dried and sieved to 2 mm. Bulk density of fine soil was measured by repeated volumetric samples (3 × 250 cm^3 per interval in general) after subtraction of the volume and weight of coarse fragments. Coarse fragments (> 2 mm for soil, > 20 mm for forest floor) were weighed after sieving and very coarse fragments (soil, > 6.3 cm) were estimated in the field. Texture was estimated in the field manually with so-called "texture-by-feel-procedure." The work of de Vos et al. (2016) indicates that it is sufficient to estimate the soil texture manually with well-trained soil scientists instead of conducting particle size analyses in the laboratory. Total C was measured by dry combustion. Inorganic C was determined by gas volumetry and OC was calculated as the difference between total and inorganic C. OC stocks were calculated by multiplying OC concentration with the stock of the fine fraction (< 2 mm for soil, < 20 mm for forest floor; Wellbrock et al., 2019).

Soil classes were determined in the field using the German classification system (Ad-hoc-Arbeitsgruppe Boden, 2005) and translated to Reference Soil Groups (IUSS Working Group WRB, 2015). Parent material was characterized in the field combining information of substrate origin and pedogenetic processes (Ad-hoc-Arbeitsgruppe Boden, 2005).

2.3 | Environmental covariates

Our model follows the widely accepted SCORPAN-approach (Arrouays et al., 2020; McBratney et al., 2003). It expands on the state factor theory of Jenny (1941) using soil properties (S), climate (C), organisms (O), relief (R), parent material (P), age (A), and space (N) as covariates for predictive soil modeling. We did not directly include covariates for the factors relief, age, and space. Relief was not included, because its effect was already captured by the profiles in the soil map (Heitkamp et al., 2020). Age was unknown, but we assumed no major differences throughout Hesse. The impact of space was tested (see below). An overview of the used covariates is given in Table 1. Climate data were regionalized to the centroids of the units of the soil map of Hesse. Briefly, daily temperature and precipitation data of the climate stations of the German Meteorological Service (Deutscher Wetterdienst, DWD) was interpolated using ordinary kriging (precipitation) and generalized additive models (temperature, using elevation and spatial coordinates). Elevation was taken from the digital elevation model with 25 m resolution (DEM25). Daily data from the period 1971 to 2000 was aggregated to mean annual temperature (MAT) and precipitation (MAP). The period was chosen since it is the current baseline for regional climate change scenarios (Hübener et al., 2017). Total atmospheric nitrogen deposition was taken from Schaap et al. (2015) using a grid resolution of 1 × 1 km. Spatial distribution of forest types (broadleaf, mixed, coniferous) was available from the "Amtliches Topographisch-Kartographisches Informations system" (ATKIS; HVBG, 2018).

All other used covariates were either determined during the NFSI or extracted from the Hessian soil map (scale 1:50,000; Hessisches Landesamt für Naturschutz, Umwelt und Geologie, 2018). If available, using point information of the NFSI for model parametrization was preferred over spatial information due to issues with generalization or positioning. The soil map contains 1143 generalized soil profiles under forest (as defined by ATKIS). Each profile informs about soil depth (maximum 200 cm), genetic horizons, and parent material, as well as classes of coarse fragments, bulk density, organic matter content, and texture according to the German classification scheme (Ad-hoc-Arbeitsgruppe Boden, 2005). Soil classes were translated into Reference Soil Groups (IUSS Working Group WRB, 2015) and parent material from the NFSI was converted into the Hessian classification (Heitkamp et al., 2020). Podzolization was derived from horizon symbols indicating different degrees of leaching of organic matter from the A-horizon, accumulation of organic matter in the B-horizon, and the presence of sesquioxides. Classes of coarse fragments and texture were converted into numerical values by using the class midst. Potential cation exchange capacity (CEC_{pot}), was used as a surrogate for soil texture, and was calculated for the NFSI and soil map profiles as:

$$CEC_{pot}(cmol_c kg^{-1}) = 0.5\,clay(\%) + 0.05\,silt(\%) + h, \quad (1)$$

where h is the organic matter class (classes: h0–h6), resulting in an addition of 0, 0, 3, 7, 15, 25, and 50 $cmol_c\ kg^{-1}$ (Bug et al., 2020).

TABLE 1 Utilized variables for model development of forest floor C stocks (FF) and mineral SOC profile (MI). Note, that some variables where only used to calculate covariates of the model. Values are the range of the data and values in brackets indicate the median

		Source/method		Data range	
Covariate	**Model**	**NFSI**	**Spatial**	**NFSI**	**Soil map**
Climate	FF/MI	Regionalization of DWD data		MAT: 4.7–10.5 (8.7) MAP: 458–1554 (722)	MAT: 5.2–10.6 (8.2) MAP: 537–1385 (760)
N deposition	FF	Schaap et al. (2015)		10.6–34.7 (15.8)	9.9–23.5 (15.7)
Forest type	FF/MI	Field	ATKIS	3 levels	3 levels
Parent material	FF/MI	Field	Map	9 levels	8 levels
Soil class	FF/MI	Field	Map	10 levels	10 levels
Soil horizons	Calc	Field	Map	–	–
Podzolization	FF/MI	Calc		6 levels (p1–p6)	4 levels (p1–p3, p6)
Organic matter class	Calc	Calc	Map	7 levels (h0–h6)	7 levels (h0 – h6)
Coarse fragments	MI	Field, Lab	Map	0–90 (5.2)	0 – 90 (13.1)
Texture	Calc	Field	Map	Sand: 3–92.5 (44.2) Silt: 4.9–89.0 (31.6) Clay: 2.5–80.3 (12.0)	Sand: 2.8 – 92.5 (21.6) Silt: 4.5 – 87.8 (52.7) Clay: 2.3 – 84.8 (14.3)
CEC_{pot}	MI	Calc		1.5–70.8 (11.7)	1.5–80.2 (13.5)

Abbreviations: DWD data, German Meteorological Service (Deutscher Wetterdienst, DWD); Field, field data of the NFSI (Wellbrock et al., 2019); ATKIS, Amtlich Topografisches Kataster Informationssystem (HVBG, 2018); Map, soil map of Hesse, scale 1:50,000 (Hessisches Landesamt für Naturschutz, Umwelt und Geologie, 2018); Lab, lab data of the NFSI (Wellbrock et al., 2019); Calc., either calculated from, or used to calculate another covariate (details see text).

2.4 | Data treatment

NFSI profiles, which do not occur as units in the Hessian soil map, *e.g.*, Treposols, or Plaggic Anthrosols, were excluded from the analysis. In addition, profiles with histic horizons were excluded, because involved processes of OC storage are very different from mineral horizons. In total, 25 from the 380 available NFSI profiles were excluded (final n = 355 profiles for forest floor and down to 90 cm mineral soil).

All numeric variables (mineral soil) were subjected to equal-area splines to obtain 5 cm depth increments using the function "mpspline" of the R package GSIF 0.5–5.1 (Hengl et al., 2019). Equal-area splines preserve the mean value of the property of interest within the sampled depth increment and redistribute the value within the sampled depth using information from above and below the layer (Bishop et al., 1999). A detailed discussion on the methodology is given by Hartemink and Minasny (2016), and Malone et al. (2009). The shape of the function is controlled by the parameter λ, which determines the trade-off between the goodness of fit and the roughness of the spline. The goodness of fit was determined by re-calculating the splined value to the original depth increment of the sample. We observed that low λ gave apparently better fits, but resulted in unrealistic depth sequences in case of large differences between observed layers (producing overshoots). This was a larger issue for texture, because of huge differences in case of multilayered parent material. The chosen λ values were 0.05, 0.05, 0.01, and 0.5 for SOC concentration, bulk density, coarse fragments, and texture (sand, silt, and clay), respectively. When sand, silt, and clay did not sum up to 100% we applied an error correction with a mass balance. This was a minor issue, with errors mostly occurring at decimal places (25 and 75% quantile = 100%). The most extreme sums were 96% and 105%. SOC stocks were calculated for five cm depth increments. SOC stocks and concentrations of sand, silt, clay, and coarse fragments of the 5 cm increments were recalculated to the original sampling depths and evaluated by linear regression ($R^2 > 0.99$, |intercept| < 0.5% of maximum, slope = 1.00). Each profile in the mineral soil consisted of a maximum of 18 (NFSI, 90 cm) or 20 (soil map, 100 cm) depth increments.

2.5 | Model parametrization and validation

Due to our available spatial data, models should be able to handle non-normal distributions, non-linear relationships, as well as categorical variables. Generalized additive models (GAM; Wood, 2017) meet these criteria. GAMs base on the construction of flexible, potentially non-linear smooth functions, which relate to the predictor. This is an advantage in 3D modeling. Other approaches have to develop separate depth functions and predict their parameters into space or model each layer separately. This step is unnecessary with GAMs, as depth can be used as a global smooth term, which allows for the prediction of continuous depth functions combined with soil-forming factors (SCORPAN) in a single model. Recently, Pedersen et al. (2019) presented the approach of hierarchical GAMs (hGAM), which introduced the inclusion of group-specific effects into the GAM framework. Group-specific effects modulate the shape of the global function. This is an attractive model property, as some factors may not change so much the total OC stock (*i.e.*, the integral of the added smooth functions), but rather the distribution among depth (*i.e.*, the shape of the depth smooth function). Therefore, hGAMs (Pedersen et al., 2019) were chosen for modeling the 3D distribution of SOC stocks in forest soils of Hesse.

The hGAMs were run with the package mgcv in R 3.6.2 (R Core Team, 2017; Wood, 2019). The smoothing parameter *k* determines the wiggliness of the smooth functions. If *k* is too high there is a risk for overfitting and if *k* is too low a part of the variation in the data may not be captured well. The optimal value for the smoothing parameter *k* was adjusted by comparing *k'* with the estimated degrees of freedom (edf) given by the command *gam.check*. Furthermore, model improvement was checked by comparing AIC values and the smooth for partial effects was checked visually. Residuals of the models were checked for normality and randomness, and results were evaluated for goodness-of-fit and quality (AIC). The residuals (*e(s)*) were also checked for spatial auto-correlation by using a mixed GAM in the form:

$$\begin{aligned} &e(s) \sim s(x, y), \\ &\quad random = list(id \sim 1), \\ &\quad family = gaussian(link = \text{“identity”}) \end{aligned} \tag{2}$$

where *x* and *y* are spatial coordinates, and id is the identifier for the individual profile. This takes care of the (non-spatial) auto-correlation within each profile (the depth increments).

2.5.1 | Model formulation and knowledge-driven variable selection for OC stocks in the forest floor

Processes affecting FFC stocks are different, at least in their effect sizes, from processes in the mineral soil. It was therefore not reasonable to predict forest floor and mineral soil stocks in a single model. Soil class and podzolization mainly reflect acidity state and water dynamics. Forest type indicates the different decomposability of incoming litter. MAT and MAP both affect plant productivity and decomposition dynamics (Djukic et al., 2018; Etzold et al., 2020). This is modulated by the type of parent material, which affects water dynamics, acidity, and biotic activity. Nitrogen deposition is related to plant productivity and was reported to decrease the speed of decomposition at the later stage (ca. 30% mass loss; Berg, 2014; Etzold et al., 2020). Finally, the month of sampling time simply reflects the annual dynamics within the forest floor due to litterfall and decomposition. A gamma distribution with log-link was used to account for the properties of the FFC data. The R-code for the final model with 23 model degrees of freedom and 329 residual degrees of freedom was:

$$\begin{aligned} &ffc\_tha \sim \\ &\quad soilclass\_g + \\ &\quad soilclass\_g + \\ &\quad forest + \\ &\quad te\left(mat\_c,\ map\_mm,\ k = 3,\ bs = c(\text{“tp”}, \text{“tp”})\right) + \\ &\quad te\left(mat\_c,\ map\_mm,\ by = pamat,\ k = 3, bs = c(\text{“tp”}, \text{“tp”}),\ m = 1\right) + \\ &\quad s\left(month, k = 4,\ bs = \text{“cc”},\ m = 2\right) + \\ &\quad s\left(ndep\_kghay,\ k = 3,\ bs = \text{“tp”}, m = 2\right), \\ &family = Gamma(link = \text{“log”}),\ method = \text{“REML”} \end{aligned} \tag{3}$$

where *ffc_tha* is the OC stock in the forest floor (t ha^{-1}), *soilclass_g* is the grouped soil class (Ad-hoc-Arbeitsgruppe Boden, 2005), *podsol_g* the grouped degree of podzolization, forest is the forest type (broadleaf, coniferous, mixed), *mat_c* and *map_mm* are the MAT (°C) and MAP (mm y^{-1}), month is the month of sampling (1–12), *ndep_kghay* is the N deposition (kg ha^{-1} y^{-1}), and *pamat* is the class of parent material. For further details regarding the implementation of R code, see Pedersen et al. (2019) and for technical model terms (*s*, *te*, *k*, *bs*, *tp*, *m*, *cc*, *by*) refer to Wood (2019). After running the model, some levels of the covariates soil class and degree of podzolization were summarized, because their effect sizes were rather similar. Degree of podzolization was classified into absent (p1), intermediate (p2–5), and strong (p6). The 10 soil classes were classified into five groups: BC (Braunerde/Cambisol, and Terrae calcis), TY (Schwarzerden/Chernozem and colluvial Anthrosol), DLR (Pelosol/Vertisol, Parabraunerde/Luvisol, and Ah/C-Böden/Leptosol), P (Podzol), and GS (Gley/Gleysol, and Pseudogley/Stagnosol).

2.5.2 | Model formulation and knowledge-driven variable selection for OC stocks in the mineral soil

Climate was incorporated as the two-dimensional smooth function of MAT and MAP and affects plant productivity and decomposition of SOC. The effect of soil texture is well known and we used CEC_{pot} as a derivate for the intercorrelated variables sand, silt, and clay. Since we modeled SOC stocks as opposed to concentrations we incorporated the volume percentage of coarse fragments. Soil depth (the top of the increment) was used as a global smooth and the function was modulated by group-specific effects of soil class, degree of podzolization, parent material, and forest type. Soil classes mirror several processes that potentially affect depth distribution. Translocation and transformation processes may alter the depth or capacity of SOC storage. Luvisols, for example, are characterized by clay migration (partly covered by changes in CEC_{pot}) induced by pH gradients. Depth distributions of Gleysols and Stagnosols are affected by their water dynamics. Effects of the degree of podzolization are associated with the presence of sesquioxides, pH effects, and organic matter redistribution. Parent material reflects the effects of nutrient availability, pH, and biotic activity. The forest type potentially affects depth distribution of SOC by differences in rooting systems and depth, varying incorporation of litter, fine root turnover, and also by affecting the soil pH. A gamma distribution with log-link was used to account for the properties of the SOC data. The R-code for the final model with 89 model degrees of freedom and 6085 residual degrees of freedom was:

$$\begin{aligned} &soc\_tha \sim \\ &\quad te\left(mat\_c,\ map\_mm,\ k = 5m = 2,\ bs = \text{“tp”}\right) + \\ &\quad s\left(cecpot\_cmolckg,\ k = 5,\ m = 2,\ bs = \text{“tp”}\right) + \\ &\quad s\left(skel\_vproz,\ k = 5,\ m = 2,\ bs = \text{“tp”}\right) + \\ &\quad s\left(top,\ k = 5,\ m = 2, bs = \text{“tp”}\right) + \\ &\qquad s\left(top,\ soilclass,\ k = 5,\ m = 2,\ bs = \text{“fs”}\right) + \\ &\qquad s\left(top,\ podsol,\ k = 5,\ m = 2,\ bs = \text{“fs”}\right) + \\ &\qquad s\left(top,\ pamat,\ k = 5,\ m = 2,\ bs = \text{“fs”}\right) + \\ &\qquad s\left(top,\ forest,\ k = 5,\ m = 2,\ bs = \text{“fs”}\right), \\ &family = Gamma\left(link = \text{“log”}\right),\ method = \text{“REML”} \end{aligned} \tag{4}$$

where *soc_tha* is the SOC stock (t ha^{-1}), *mat_c* and *map_mm* are the MAT (°C) and MAP (mm y^{-1}), *cecpot_cmolckg* is the potential cation exchange capacity ($cmol_c$ kg^{-1}), *skel_vproz* is the content of coarse fragments (vol.%), *top* is the upper border of the depth increment (cm), *soilclass* is the soil class (Ad-hoc-Arbeitsgruppe Boden, 2005), *podsol* is the degree of podzolization, *pamat* is the class of parent material, and *forest* is the forest type (broadleaf, coniferous, mixed). For further details regarding the implementation of R code, see Pedersen et al. (2019) and for technical model terms (*s*, *te*, *k*, *bs*, *tp*, *m*, *cc*) refer to Wood (2019).

2.5.3 | Validation

Model validation follows the suggestions of Kempen et al. (2018). Internal model quality measures were calculated with the parametrization dataset. We also tested our models with a 10-fold cross-validation procedure. For this purpose, the data were randomly partitioned into 10 parts ("folds"), nine parts for model training and one part for evaluation of predictions. The folds were subsequently switched, so that each fold was used as test and training test. The base for randomly selected training and prediction sets were individual profiles (not datapoints), since depth increments within one profile are auto-correlated (Nauman and Duniway, 2019). Ten-fold cross-validation was repeated 10 times in order to get an idea of model stability. Since the Reference Soil Groups Pelosol and Chernozem were present with only one and two profiles, respectively, they had to be excluded from cross-validation (n = 352 profiles).

Following Kempen et al. (2018) we present four quality measures, which all base on the prediction error e at location s:

$$e(s) = \hat{Z}(s) - Z(s), \tag{5}$$

where $\hat{Z}(s)$ is the predicted and $Z(s)$ the observed value at location s. Prediction errors followed a normal distribution around zero. The mean error (ME) is a measure for systematic bias and was calculated as the mean of $e(s)$. Negative values of ME indicate systematic underestimation by the model and vice versa. Mean absolute relative error (MARE) and root mean squared error (RMSE) are measures for accuracy. The MARE is the mean of $|e(s)|$ expressed as the portion of the mean of OC stocks. MARE indicates the relative mean difference of predictions and observations. Using the RMSE gives higher emphasis on extreme deviations between predictions and observations. Both MARE and RMSE indicate congruity of prediction and observation at zero with increasingly worse fits with increasing values. The amount of variation explained (AVE), also called model efficiency, is roughly analogous to R^2 values. A value of zero means that the prediction is as good as the observed mean value of the population. Negative values indicate that the mean is a better predictor, and a value of one indicates congruence of predicted and observed values. AVE was calculated as:

$$AVE = 1 - \frac{\sum_{i=1}^{N}\left(\hat{Z}(s_i) - Z(s_i)\right)^2}{\sum_{i=1}^{N}\left(Z(s_i) - \bar{Z}\right)^2}. \tag{6}$$

2.6 | Sensitivity analysis

The mgcv package offers visualization of partial effects of the GAM. This is useful and informative when familiar with GAMs. However, the interpretation of additive effects at log-scale in combination with the hierarchical approach is not always straightforward. Hierarchical partial effects alter the shape of the global smoother. This allows some interpretation of the relative effect in the model, but impedes interpretation of the effect on OC stocks in the original unit (t ha^{-1}). Therefore, we decided to present standardized SOC stock profiles and FFC stocks. We conducted a standard sensitivity analysis by varying only one covariate of interest at a time, and keeping all the other covariates constant (Guckland et al., 2012). Numerical covariates were kept at the median of the whole dataset (Table 1), whereas the most common class was used for categorical covariates. Then, OC stocks were predicted across the depth gradient and presented with their 95% confidence intervals (CI). The standard errors (log-scale) from the 5 cm-wise predicted C stocks (log-scale) were multiplied by 1.96 to obtain CIs. The log-values were added or subtracted from the predictions and then back-transformed to the original scale. Note that this results in asymmetric CIs. Since climatic effects on OC stocks were modeled by the two-dimensional smooth function of MAP and MAT, we present the full effect range only for 0–5 cm (mineral soil) and exemplify the effect of MAT at a given MAP for the full depth. For the forest floor, two contrasting parent materials are presented. This approach aimed to test the effect strength of individual covariates, rather than to produce realistic profiles or environmental combinations.

2.7 | Spatial prediction and uncertainty

The soil map polygons were merged with the ATKIS layer to include information about the forest type. This resulted in a finer division of polygons as given in the original soil map, but borders were preserved (Heitkamp et al., 2020). Information of the other spatial layers for model variables (MAT, MAP, N deposition; Table 1) was extracted using their center of mass (centroids inside the polygons) of the ATKIS-soil map. Each soil map polygon is related to one of the 1143 soil profiles (Section 2.3), which was prepared for the predictions as described above (Section 2.4). OC stocks were then predicted to the soil map profile data at the log-scale including standard errors. Predictions were done for the forest floor (assumed sampling month: June) and 5 cm depth intervals down to 100 cm. This is a small extension in comparison to the parametrization set (0–90 cm). Although slightly outside the parameter range, we judged this as acceptable to obtain results for the standard depths of 100 cm. Results were transformed to the original scale. Profiles with histic horizons or anthropogenic substrate were excluded from the predictions. This was about 0.33% of the total forest area. Overall, predictions were made for 194,879 mapped soil units and 3,897,580 data points (soil units including depth increments) for an area of 8669 km^2. Predicted data for the whole area of Hesse were aggregated across depth increments for a better overview. Chosen strata are (a) forest floor and mineral soil, (b) division of the mineral

soil into top and subsoil (0–30 cm, 30–100 cm), and (c) standard depth increments of the global soil map (0–5 cm, 5–15 cm, 15–30 cm, 30–60 cm, and 60–100 cm).

Model validation results in measures of the overall performance of the model (Kempen et al., 2018). In contrast, uncertainty is spatially explicit (Heuvelink, 2018). There are several sources of uncertainty. However, a complete uncertainty analysis is beyond the scope of this manuscript and total uncertainty is probably larger (see Discussion). Here, we present solely structural model uncertainty (*sensu* Heuvelink, 2018) without explicitly taking attribute, positional, and covariate uncertainty into account. Structural model uncertainty is presented either as the range of the 95% CI or as the margin of error (95% confidence level), using error propagation rules for summation of depth increments (for calculation see 2.6). Due to asymmetric CIs, the upper and lower boundaries of the margins of error differ. The margin of error is defined as the difference between the predicted value and the highest (upper boundary) or lowest value (lower boundary) of the 95% CI. The margin of error is expressed as a relative value for the depth increments to provide better comparability between them.

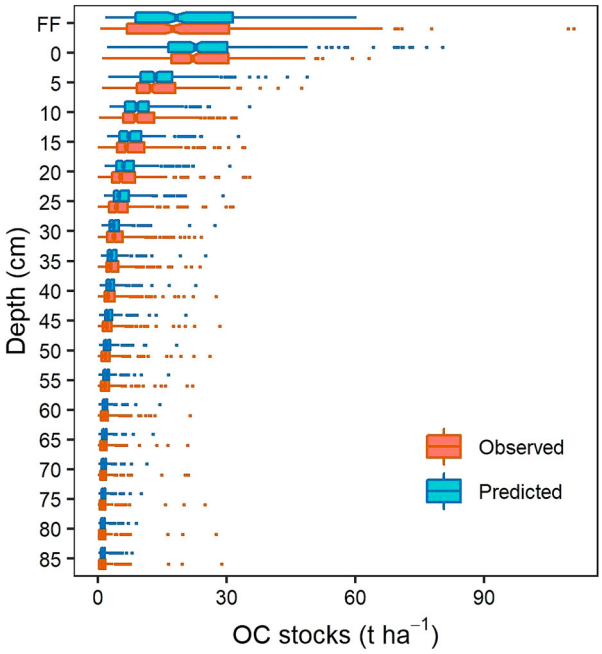

FIGURE 1 Boxplots of OC stocks in the forest floor and the mineral soil (0–90 cm). Observations and predictions of the combined NFSI datasets of Hesse, Lower Saxony, and Saxony-Anhalt (n = 355 profiles). Depth represents the upper border of the increment. FF: Forest floor; Line: median; Box: interquartile range (IQR); whiskers: up to 1.5 × IQR + 75th percentile or 25th percentile; points: potential outliers outside of whisker range; notches: median ± 1.58 × IQR / $\sqrt{n}$

3 | RESULTS

3.1 | Carbon stocks of the NFSI

Figure 1 presents the observed and predicted forest soil OC stocks from the forest floor down to 85–90 cm of the three federal states Lower Saxony, Saxony-Anhalt, and Hesse (NFSI dataset). Overall, the data range of observed and predicted stocks was very similar. The interquartile range (IQR) of observed FFC stocks (t ha^{-1}) was 6.8 to 30.7 (median: 17.5). Predicted FFC stocks were slightly higher, with an IQR from 8.9 to 30.4 (median: 18.4). SOC stocks (t ha^{-1}) were highest in 0–5 cm (observed IQR: 17.2 to 30.4, median 22.1; predicted IQR: 16.5 to 30.2, median 22.7). There was a sharp decline until approximately 25–30 cm with observed and predicted medians of 4.4 and 5.0, respectively. The SOC stocks declined to minimum medians of 1.1 (observed) and 1.2 (predicted) with IQR of 0.4 to 1.8 (observed), and 0.8 to 1.6 (predicted). In general, observed extreme values (> 1.5 × IQR) were not captured very well by the predictions. Only at 0–5 cm depths, extremes of the predictions clearly exceeded the extremes of observed OC stocks.

The observed sum of SOC stocks (mineral soil 0–90 cm) ranged from 17.4 to 396.4 t ha^{-1} with an IQR of 63.9 to 119.0 t ha^{-1} (median: 84.8 t ha^{-1}). Predicted stocks were slightly higher (range of 27.8 to 411.8, median: 91.0), but had a lower IQR of 68.2 to 115.3 t ha^{-1}.

3.2 | Model performance and validation

Visual comparison between observed and predicted OC stocks showed a generally good agreement (Figure 2). All residuals were randomly distributed around zero, and showed no spatial autocorrelation (Equation 2; significance level for intercept and the term *s(x,y)* > 0.49 and adjusted $R^2 \leq 0.001$). A comparison between internal validation (parametrization) and cross-validation showed that the latter predictions performed slightly worse (Figure 3). The standard deviation between cross-validation runs was low. This indicated good stability of the models. In the following, we present the results of the cross-validation, if not stated otherwise.

Stocks of FFC showed the highest scatter (Figure 2), but no systematic bias (Table 2; ME 0.20 ± 0.07 t ha^{-1}). The RMSE was highest (13.7 ± 0.2 t ha^{-1}) with a MARE of 43 ± 0.4%. The AVE was 0.37 ± 0.02. The worst performance of the mineral soil model was observed at 0–5 cm depth. The scatter was relatively high and a subpopulation (predicted SOC stocks > 40 t ha^{-1}) was overestimated (Figure 2). This resulted in a high RMSE (9.7 ± 0.3 t ha^{-1}), a low AVE (0.12 ± 0.05), and the highest ME (1.2 ± 0.1 t ha^{-1}; Figure 3A,B,D). However, the ME was still less than 5% of the mean and the MARE one of the lowest (29 ± 0.6%) compared with the other depth increments. The overestimated sub-population (n = 14 of 355) seemed to act as a leverage point, strongly affecting calculations of RMSE and AVE. When ignoring predictions > 40 t ha^{-1} AVE increased substantially to 0.35. With increasing depth, ME became very small and the RMSE decreased (Figure 3A,B), as also the SOC stocks (Figures 1 and 2). There was generally a gradual increase of the MARE from 29% to 63% with increasing depth. The AVE (Figure 3D) showed a less directional pattern. The AVE in the mineral soil increased to a maximum of 0.57 ± 0.01 at 15–20 cm, remained relatively stable around 0.5 down to 40–45 cm, and decreased afterward to 0.22 ± 0.03

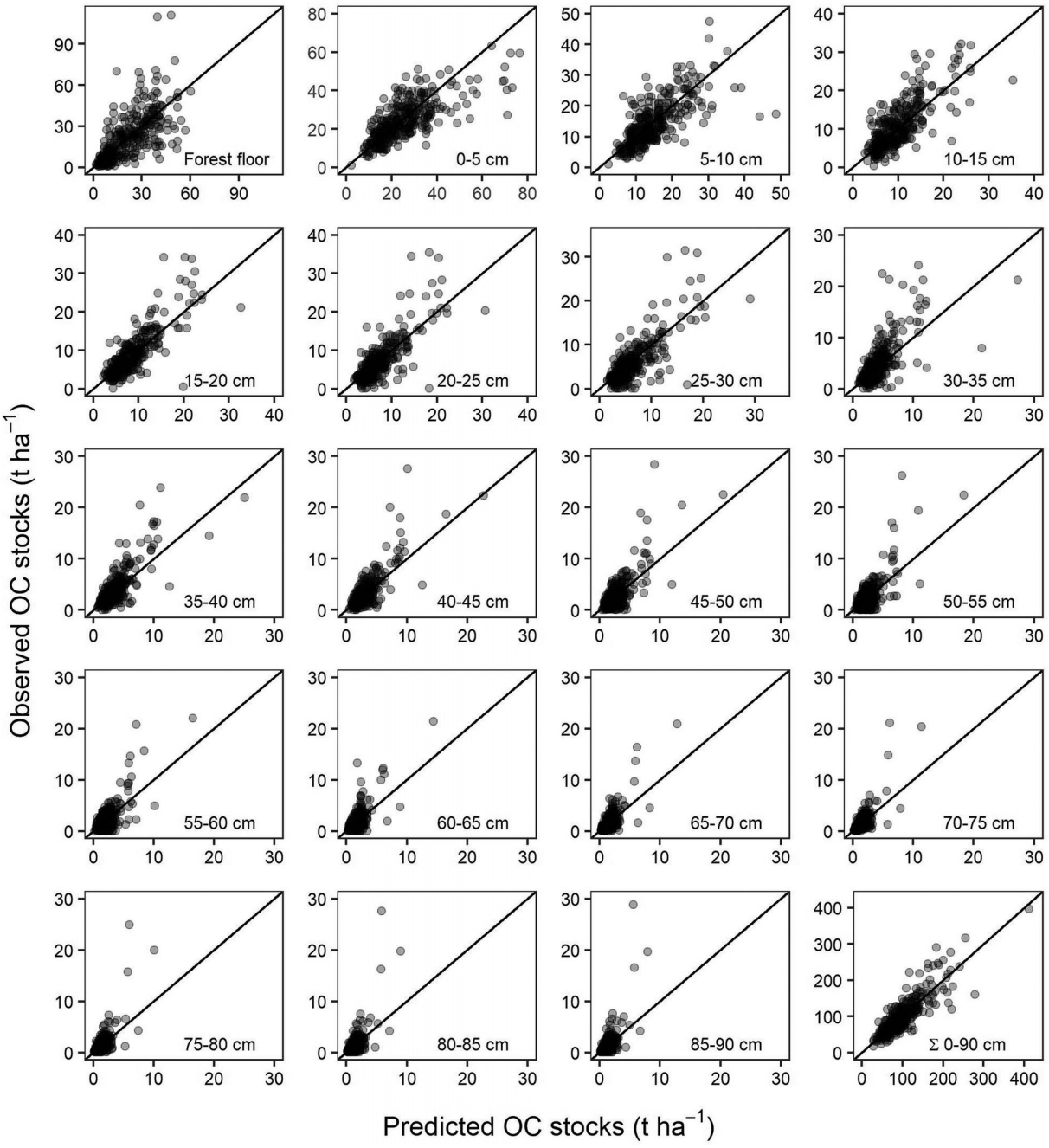

FIGURE 2 Observed and predicted OC stocks in different soil depth increments, and the sum of all mineral soil depth increments (combined NFSI dataset of Hesse, Lower Saxony, and Saxony-Anhalt, $n = 355$ profiles). Note that axes were scaled to fit the data range

at 85–90 cm. This pattern is also well reflected in the distribution of values around the 1:1 line of the scatter plots (Figure 2).

It is noteworthy that model performance for the whole dataset of the mineral soil (0–90 cm in 5 cm depth increments) was much better than for depth-wise stratification (Table 2). The total SOC stocks (Σ 0–90 cm, *i.e.*, the sum of all depth increments 0–90 cm) is scattered tightly around the 1:1 line (Figure 2). Consequently, the validation measures (Table 2) showed no systematic bias, compared to individual depth increments a low MARE (23 ± 0.4%), and a high proportion of explained variance (AVE 0.60 ± 0.02).

3.3 | Effect strength of covariates and sensitivity analysis

3.3.1 | Forest floor

The FFC stock was expected to be clearly affected by forest type. Indeed, all other factors being constant, FFC stocks under mixed forests were predicted to be 1.8, and under coniferous forest 2.4 times larger than under broadleaf forests (Figure 4A–D). Soil classes with similar effect sizes were grouped together. Colluvial soils as well as

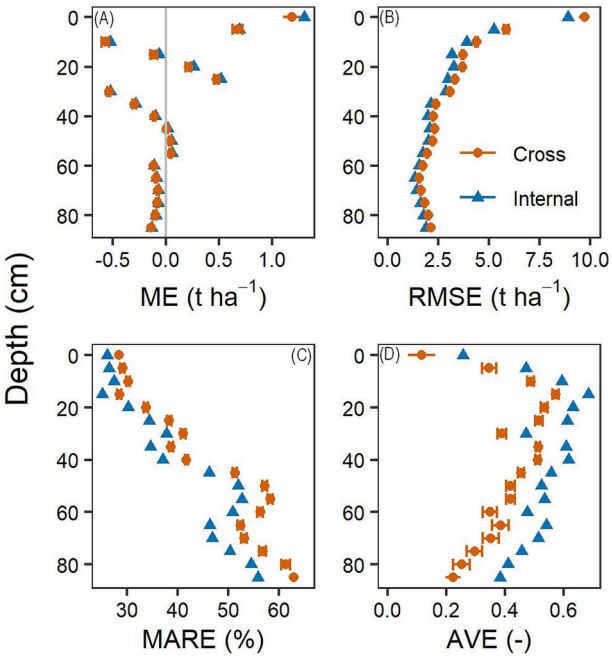

FIGURE 3 Global map quality measures from internal (parametrization) and 10-times repeated 10-fold cross-validation (cross, means, and standard deviation) of the mineral soil model (NFSI dataset, $n = 355$ profiles). (A) Mean error (ME); (B) root mean squared error (RMSE); (C) mean absolute relative error (MARE); (D) amount of variance explained (AVE)

Chernozems showed the lowest FFC stocks of 2.6 and 6.2 t ha^{-1} under broadleaf and coniferous forest, respectively. Four times higher FFC stocks were predicted for water-affected soils (Gleysol and Stagnosol, 10.8 and 26.1 t ha under broadleaf and coniferous forest). With an increasing degree of podzolization (classes absent: p1; intermediate p2–p5; strong: p6) FFC stocks increased gradually by a factor of 1.8. Increasing N deposition from 10 to 35 kg ha^{-1} y^{-1} also increased FFC stocks 2.6 times. Sampling month affected FFC stocks more subtly. The minimum FFC stocks were 75% of the maximum. This was equivalent to an apparent intra-annual dynamic of 2 and 4.7 t ha^{-1} under broadleaf and coniferous forest, respectively.

The effect of climate on FFC stocks on acidic parent material was uniform across the range of MAT-MAP combinations that occur in the used datasets (Figure 4E). There was a trend toward higher FFC stocks at more cool and wet conditions. The highest FFC stocks occurred at cool (MAT approx. < 6°C) and wet (MAP approx. 900 to 1200 mm y^{-1}) conditions, whereas at very wet conditions above MAP of 1200 mm y^{-1} FFC stocks decreased again. This effect, however, occurred at the border of the parameter space. On base rich parent material, there was a much more complex effect of climate on FFC stocks (Figure 4F). The most notable difference as compared to acidic parent material occurred at low MAP, where FFC stocks were predicted to increase steeply. The lowest FFC stocks were predicted to occur at intermediate MAP and high MAT.

3.3.2 | Mineral soil

The covariates MAT-MAP combination, CEC_{pot}, and coarse fragments do not interact with the depth smoother. Therefore, their effect on SOC stocks was similar throughout the depth increments, that is, the proportion between two levels of the covariate was the same.

Climatic effects on SOC stocks were predicted to be quite complex (Figure 5A,B). We exemplify the effect at the median of MAP of 760 mm y^{-1} for a temperature gradient at 0–5 cm. At 7.3°C SOC stocks were highest (13.3 t ha^{-1}) and decreased by 3.7 t ha^{-1} at 7.8°C. A further increase of MAT to 8.2°C led to predicted SOC stocks of 8.9 t ha^{-1}. Then, SOC stocks increased again to 10.2 t ha^{-1} with a further increase in temperature to 8.7°C. At the given MAP a further increase of 1 t ha^{-1} was predicted for a MAT of 9.3°C. The polygons (Figure 5B) indicate the data range of MAT and MAP in the NFSI dataset and the map of Hesse. It shows that the map contains combinations of MAT and MAP, which were not covered by the parametrization dataset. These results have to be handled with care (see discussion). The effect of CEC_{pot} on SOC stocks was very pronounced (Figure 5C). At 0–5 cm only 2.9 t SOC ha^{-1} were predicted with a CEC_{pot} of 1.5 $cmol_c$ kg^{-1}. SOC stocks increased up to 18 t ha^{-1} with a CEC_{pot} of 70 $cmol_c$ kg^{-1}. Compared to the absence of coarse fragments, SOC stocks decreased to 89% and 75% at 10% and 25% of coarse fragments, respectively (Figure 5D). This mirrors almost perfectly the effect of coarse fragments in SOC stock calculation. The decrease in SOC stocks with increasing shares of coarse fragments was not proportional. At 50% and 90% of coarse fragments SOC stocks were 58% and 17% of the maximal stock without coarse fragments, respectively.

The covariates soil class, podzolization, parent material, and forest type were included as hierarchical effects of the global smoother for soil depth. Predicted SOC stocks for different soil classes did not

TABLE 2 Global map quality measures from internal (parametrization) and cross-validation for the forest floor (FF), all depth increments (0–90 cm), and the sum of the SOC stocks of the mineral soil (Σ 0–90 cm). Values for the 10-fold cross-validation are means with standard deviations of 10 replications

	Internal validation				Cross-validation			
Layer	ME (t ha^{-1})	MARE (%)	RMSE (t ha^{-1})	AVE (–)	ME (t ha^{-1})	MARE (%)	RMSE (t ha^{-1})	AVE (–)
FF	0.19	39	12.40	0.49	0.21 (0.07)	43 (0.4)	13.71 (0.16)	0.37 (0.02)
0–90 cm	0.05	32	3.32	0.79	0.03 (0.02)	36 (0.3)	3.69 (0.05)	0.74 (0.01)
Σ 0–90 cm	0.89	19	25.40	0.74	0.46 (0.33)	23 (0.4)	31.60 (0.60)	0.60 (0.02)

Abbreviations: ME, mean error; MARE, mean absolute relative error; RMSE, root mean squared error; AVE, amount of variance explained.

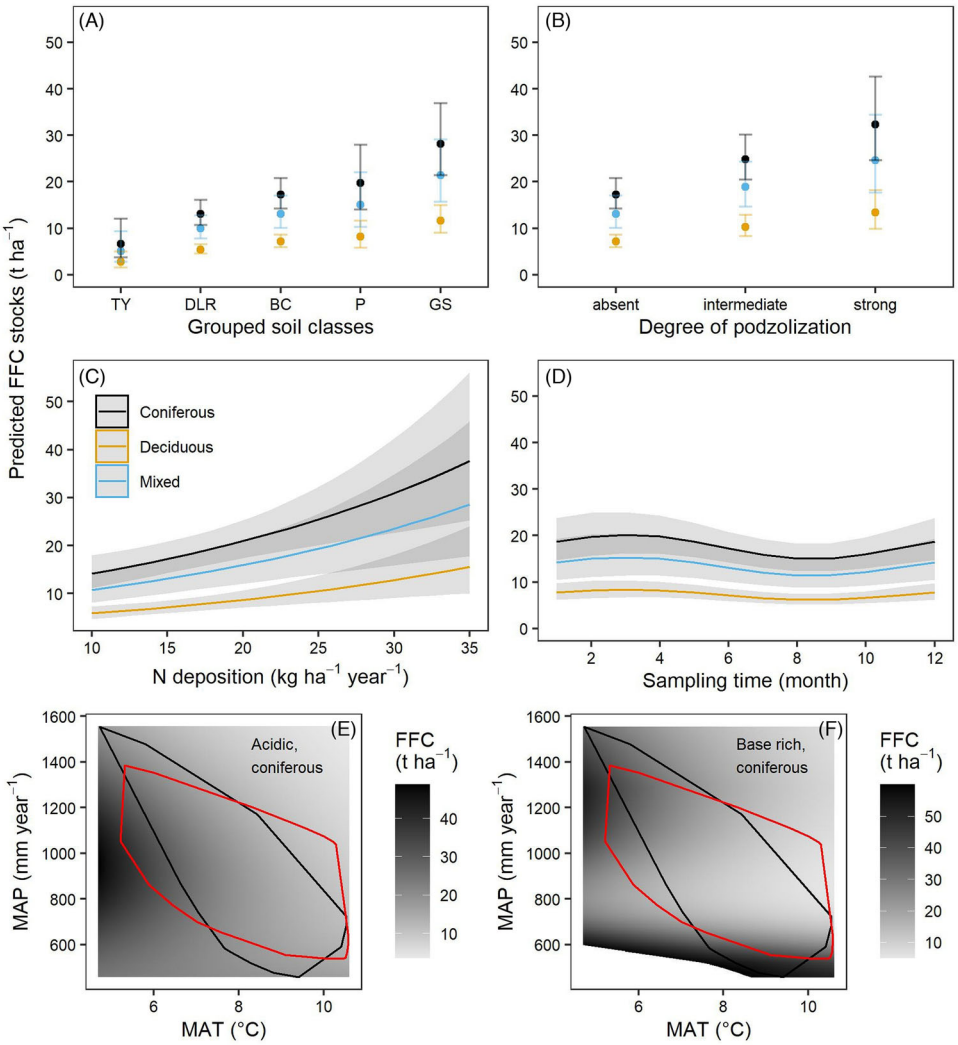

FIGURE 4 Selected examples for the covariates' sensitivity of the forest floor model. The covariate of interest varies, whereas the other covariates are set to the median values of the spatial datasets (see Table 1), or the dominant category (soilclass: Cambisol; degree of podzolization: absent; parent material: base poor). The shaded area or the error bars represent the 95% confidence interval. The interaction of MAT and MAP is given for acidic and base rich parent material. The black polygon is the data coverage of the NFSI dataset and the red polygon is the data coverage of the spatial dataset. FFC: forest floor carbon (t ha^{-1}); MAT: mean annual temperature (°C), MAP: Mean annual precipitation (mm y^{-1}); grouped soil classes: TY (Chernozem/Schwarzerde and colluvial Anthrosol), DLR (Vertisol/Pelosol, Luvisol/Parabraunerde, and Leptosol/Ah/C-Böden), BC (Cambisol/Braunerde and Terrae calcis), P (Podzol), and GS (Gleysol/Gley and Stagnosol/Pseudogley); Degree of podzolization: absent (p1), intermediate (p2–5), and strong (p6)

vary widely. Predicted SOC stocks for the whole profile (0–100 cm, range of 95% CI) of the five selected soil classes Luvisol, Cambisol, Stagnosol, Gleysol, and Podzol were 51–55, 56–60, 55–60, 56–63, and 70–76 t ha^{-1}, respectively. However, soil class had the largest effect on the depth distribution of SOC (Figure 5E). Gleysols had the lowest SOC stocks at the surface, but were predicted to store higher amounts at deeper parts of the profile. Highest SOC stocks at the top were found in Stagnosols, which had in turn lower stocks in lower-profile parts. Luvisols had, compared to other soil classes, the lowest stocks approximately at a depth of 15–30 cm. Podzols were predicted to show high SOC stocks in the upper third of the profile. The effect of podzolization was not as straightforward as expected (Figure 5F). The degrees p1 and p3 did not differ in their size and depth distribution, and the lowest stocks were predicted. The highest stock at the top of the profile was predicted for p4, followed by p6 and p2. The most notable difference in depth distribution of SOC in regard to parent material was predicted between acidic and base rich (Figure 5G). Soils with acidic parent material showed higher SOC stocks at the top compared to base rich soils. This was reversed at ca. 40 cm depths. Soils originating from eolic sand or fluviatile parent material were predicted to have higher SOC stocks that cannot be explained by other covariates throughout the profile (see Discussion). The effect of forest type was generally very small (Figure 5H). Mixed stands showed slightly higher stocks at the top and this was reversed in the lower part of the profile.

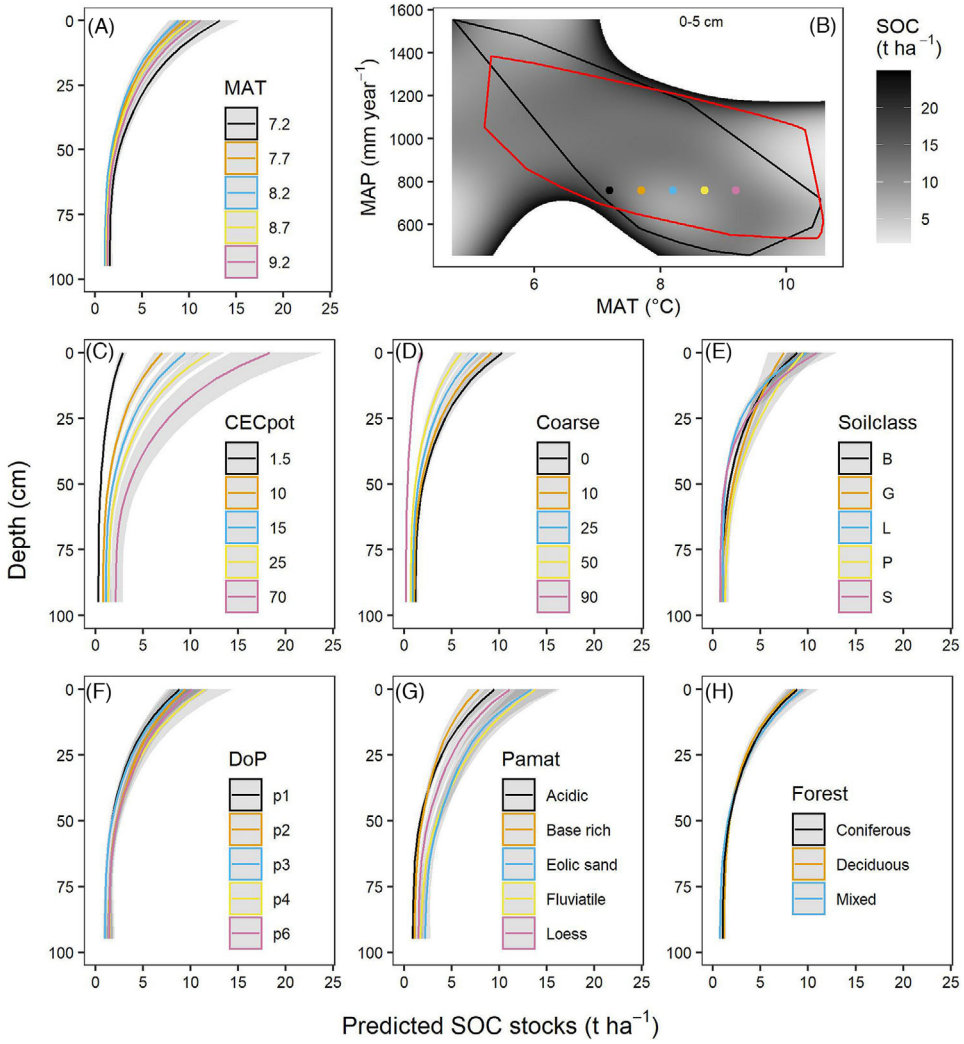

FIGURE 5 Standardized SOC profiles to evaluate the covariates' sensitivity of the mineral soil model. The covariate of interest varies as given in the legend, whereas the other covariates are set to the median values of the spatial datasets (see Table 1) or the dominant category (soil class: Cambisol; degree of podzolization: p1; parent material: base poor, forest type: coniferous). The shaded area is the 95% confidence interval. The interaction of MAT and MAP is given for the 0–5 cm depth increment (B). The dots within the surface plot (B) indicate the values given in the depth profile for MAT (A). The black polygon is the data coverage of the NFSI dataset and the red polygon is the data coverage of the spatial dataset. SOC: soil organic carbon (t ha^{-1}); MAT: mean annual temperature (°C), MAP: Mean annual precipitation (mm y^{-1}); CECpot: potential cation exchange capacity (cmol$_c$ kg^{-1}); Coarse: Coarse fragments (> 2 mm, vol.%); DoP: Degree of podzolization; Pamat: Parent material; Soil classes: B: Cambisol/Braunerde, G: Gleysol/Gley, L: Luvisol/Parabraunerde, P: Podzol/Podsol, S: Stagnosol/Pseudogley

3.4 | Spatial distribution of carbon stocks and uncertainty

Regarding the spatial distribution (histograms in Figure 6), about 25% of the forested area had OC stocks of 50 to 70 t ha^{-1}, the majority (35%) were in the class of 70 to 90 t ha^{-1}, and 20% between 90 and 100 t ha^{-1} (Figure 6A). The highest OC stocks (> 110 t ha^{-1}) were predicted in mountainous areas, groundwater-affected locations (Gleysols), or depressions. The mineral soil OC stocks largely resembled this pattern, however on a lower level (Figure 6B).

The mountain areas were also characterized by the largest uncertainty (Figure 7). The upper margin of error of the Rhön Mountains (East), the Vogelsberg (center), parts of the Rhenish Massif (North-West), and the Odenwald (South) was mostly > 21 t ha^{-1} (lower margin > 15 t ha^{-1}). Especially for the Vogelsberg, uncertainty for mineral soil stocks without FFC was considerably smaller (margins of error of 6 to 12 t ha^{-1}). Uncertainties in the mineral soil remained large for the Rhön Mountains, the Odenwald, and also parts of the Rhine Plains (South-West). Almost 70% to 80% of the forest area showed margins of error of 3-9 t ha^{-1} for total stocks, and for mineral SOC stocks margins of error of < 6 t ha^{-1}.

The spatial distribution of OC stocks in the depth increments (Figure 6C–F; forest floor, 0–5 cm, 50–55 cm, and 95–100 cm) was generally right-skewed. The flattest distribution was predicted for the

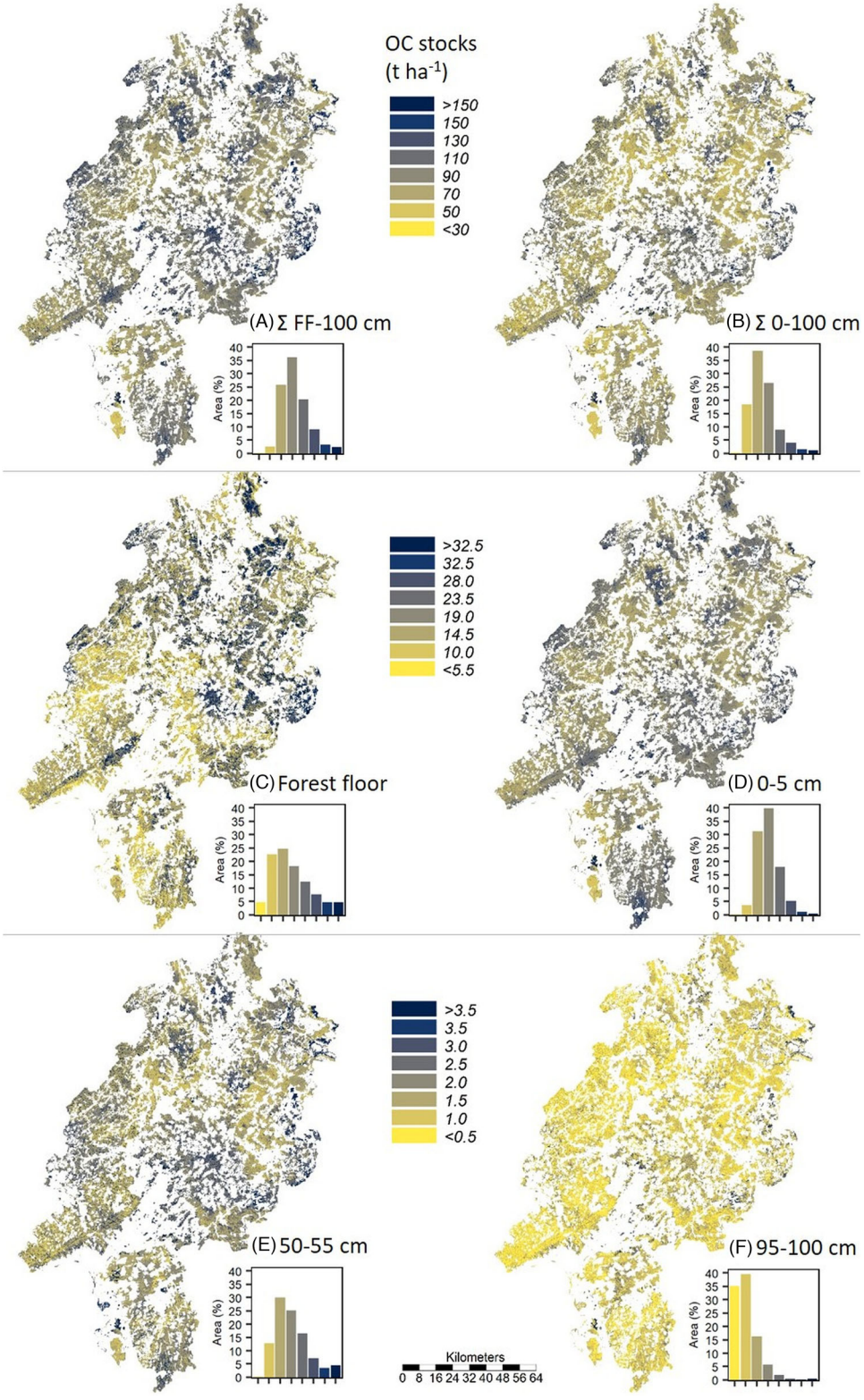

FIGURE 6 Maps of predicted OC stocks for (A) the whole profile from the forest floor (FF) to 100 cm depth, (B) the sum of the mineral soil (0–100 cm), (C) the forest floor, (D) 0–5 cm depth, (E) 50–55 cm depth, and (F) 95–100 cm depth. The inset histograms show the spatial distribution over forest soils of Hesse. Note that the two figures within each row share the same legend. Thus, there are different scales between rows, despite of the same color regimes

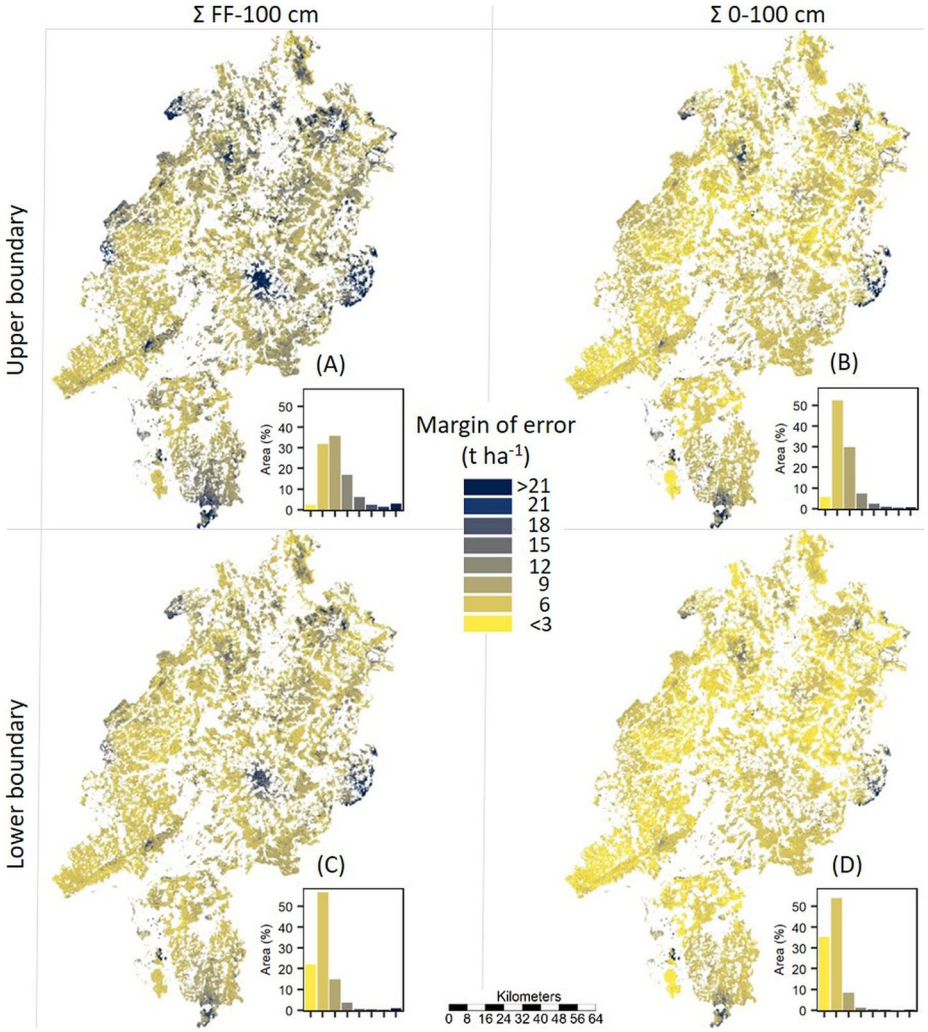

FIGURE 7 Mapped absolute model uncertainties of total OC stocks (sum of forest floor and mineral soil) and mineral soil (0–100 cm). The upper row shows the upper boundary, and the lower row the lower boundary of the margins of error (95% confidence level). The inset histograms show the spatial distribution over forest soils of Hesse. Note that upper and lower boundaries of the margins of error differ due to back-transformation from the log scale

forest floor. FFC stocks between 5.5 and 14.5 t ha^{-1} were predicted for almost half of the forest area. Considerable proportions (12.4%) had FFC stocks between 23.5 t ha^{-1} and 32.5 t ha^{-1} or even higher (4.7%). High FFC stocks were generally estimated for mountainous areas, but also when acidic parent material occurred (*e.g.*, East Hessian Highlands). Whereas the highest SOC stocks (mineral soil) were also predicted for high elevations, this was not necessarily true for acidic parent material. Within the mineral soil, there was, as expected, a steep decrease of SOC stocks with depth. At 0–5 cm, SOC stocks were between 10 and 19 t ha^{-1} at approx. 90% of the area (Figure 6). At intermediate depth (50–55 cm) two-thirds of the forested area had SOC stocks between 1 and 2.5 t ha^{-1}, and at the lowest depth, 74% of the area had less than 1 t SOC ha^{-1} (95–100 cm). Spatial distribution within the mineral soil in different depth increments was relatively uniform. That is, mountain areas or water affected soils showed high stocks throughout the profile.

Uncertainty for FFC stocks was generally high compared to other soil layers (Figure 8). Most upper margins of error were in the range of 20-60% of the modeled FFC stock (lower margins: 17 to 37%). Upper margins of error of > 100% occurred mostly at high elevations. Throughout all depth increments of the mineral soil, upper margins of error of > 100% (lower margins > 50%) were found at the Hoher Meißner (North), Rhön Mountains (East), and parts of the southern Odenwald (South). The predictions of mineral SOC stocks for the Vogelsberg (center) did not have exceptionally high uncertainty, in contrast to the forest floor. In general, uncertainty throughout the depth increments resembled the pattern of the AVE (Figure 3). At 0–5 cm, 90% of the relative upper margins of error were between 10% and 30% (lower margins: 9-23%). Uncertainty was lowest in the intermediate parts of the profiles. At 50–55 cm, 86% of the area had upper margins of error between 10% and 20% (lower margin: 9-17%). Relative uncertainty increased with depth. At 90–100 cm, 84% of the

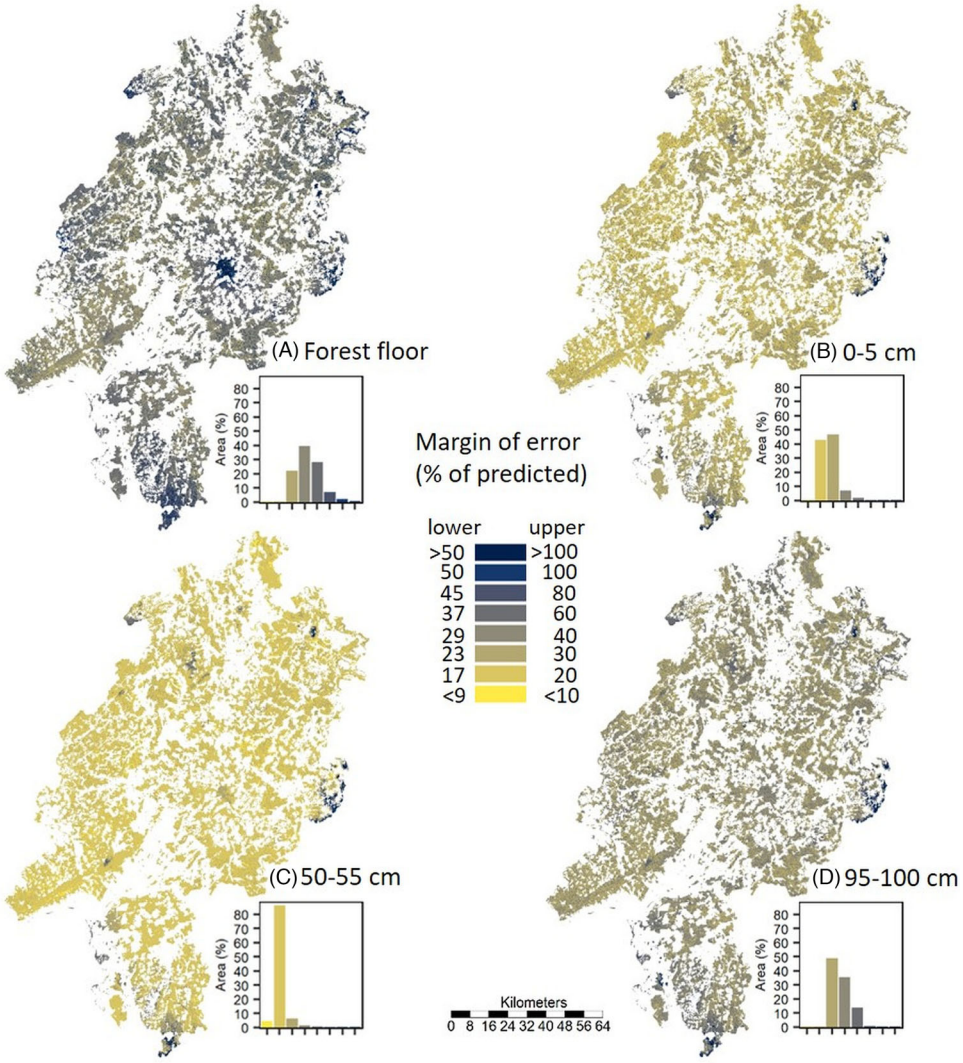

FIGURE 8 Mapped relative model uncertainties for (A) the forest floor, (B) 0–5 cm depth, (C) 50–55 cm depth, and (D) 95–100 cm depth. Upper and lower boundaries of the margins of error (95% confidence level) are given as % of the predicted value. The inset histograms show the spatial distribution over forest soils of Hesse. Note that upper and lower boundaries of the margins of error differ due to back-transformation from the log scale

upper margins of error were between 20% and 40% (lower margins: 17-29%), and 14% had upper margins of error between 40% and 60% (lower margins: 29-37%).

3.5 | OC stocks of the entire federal state

In total, forest soils of Hesse (without soils with histic horizons) were predicted to store between 67.7 and 80.1 Mt OC (range of the 95% CI; Table 3). Between 16 and 24% (10.4 to 19.9 Mt) were stored on the forest floor. The upper 30 cm of the mineral soil, often referred to as "topsoil," stored 68 to 69% of SOC, which leaves 17.6 to 19.4 Mt OC in the subsoil (30–100 cm). As area-weighted average, the total OC stocks (forest floor to 100 cm depth) ranged (95% CI) from 78.0 to 92.5 t ha-1 (Table 3). FFC stocks ranged on area-weighted average from 12.0 to 22.9 t ha^{-1} (Table 3).

4 | DISCUSSION

4.1 | Model performance

Comparing model performance with other studies is not always straightforward. Varying model approaches, different scales, prediction of concentrations or stocks, and a lack of standardized validation measures hamper direct comparisons (Lamichhane et al., 2019; Vereecken et al., 2016). The most-reported measure is probably the coefficient of determination (R^2). However, the coefficient of determination could be biased, insufficient, and misleading (Li, 2017). It is not always clear how R^2 values were achieved, for example, from a separate approach or directly from some model output, or if they refer to training or test data. Most commonly, observed and predicted values are analyzed by linear regression. Unfortunately, intercept and slope (*i.e.*, potential bias) of the regression model are seldom reported and model

TABLE 3 Vertical distribution of predicted mean and total C stocks in the forest soils of Hesse, Germany. Figures are the lower and upper boundary of the 95% confidence interval (CI) with averages given in brackets. Note that the CI was used as a measure of model uncertainty, without taking other sources (attribute, positional, or covariate, sensu Heuvelink, 2018) into account. SOC stocks and their uncertainty were aggregated from modelled 5 cm depth increments

Layer	OC stock[a] (t ha^{-1})	Total stock[b] (Mt)	Proportion (%)
Total	78.0–92.5 (84.1)	67.6 - 80.1 (72.9)	100
Forest floor	12.0–22.9 (16.5)	10.4–19.9 (14.3)	16–24 (20)
Mineral soil	63.9–72.4 (67.7)	55.3–62.7 (58.6)	76–84 (80)
Top and subsoil (mineral soil)			
0–30 cm	42.7–51.0 (46.4)	37.0–44.1 (40.2)	68–69 (69)
30–100 cm	20.4–22.4 (21.3)	17.6–19.4 (18.4)	31–32 (31)
Global soil map increments (mineral soil)			
0–5 cm	13.6–20.3 (16.5)	11.7–17.6 (14.3)	22–27 (24)
5–15 cm	13.8–17.7 (15.5)	11.9–15.3 (13.5)	23 (23)
15–30 cm	13.2–15.7 (14.3)	11.4–13.6 (12.4)	21–22 (22)
30–60 cm	12.9–14.6 (13.6)	11.1–12.6 (11.8)	19–21 (20)
60–100 cm	7.2–8.2 (7.7)	6.2–7.1 (6.6)	11–12 (11)

[a]Area-weighted mean;
[b]total sum of forested area (8690 km^2).

performance can be low despite of high R^2 values (Li, 2017; Piñeiro et al., 2008). When comparing our AVE with R^2 values from other publications, we assume that the authors presented bias-free data. In this case, AVE and R^2 measures are well comparable (Li, 2017). Achieved R^2 values in spatial modeling of OC contents or stocks were reported to range from 0.1 to 0.7, but mostly between 0.3 and 0.5 (de Brogniez et al., 2015; Gomes et al., 2019; Ma et al., 2021; Mulder et al., 2016; Nussbaum et al., 2014; Russ et al., 2021). Large-scale studies often had lower R^2 values around 0.2 to 0.3, whereas small-scale studies often reach R^2 values around 0.5 (Chakan et al., 2017; Nussbaum et al., 2014; Russ et al., 2021). Validation for depth increments often showed worse performance than the full model. The pattern of low performance at the top, best performance at intermediate depths, and again lower performance at lower-profile depths was also reported by others (Nauman and Duniway, 2019; Russ et al., 2021). Ma et al. (2021) concluded that this is a feature of sampling density and data properties and could be fixed by sampling smaller increments at the top of the profile. However, especially sampling of forest soils is challenging. Division of the forest floor and the top of the mineral soil may introduce sampling errors (Jansen et al., 2005; Russ et al., 2021). Moreover, effects of former, often unknown, management are strongest at the topmost parts of soil profiles (Poeplau et al., 2020; Springob et al., 2001). While direct management effects were reported to be minor in lower parts of soil profiles (de Vos et al., 2019), subsoil sampling, and modeling inherits its challenges. The tendency of higher coarse fragments concentration combined with low OC concentrations introduces higher uncertainty in sampling and measurement (Throop et al., 2012). A special challenge is posed by polygenesis (Richter and Yaalon, 2012). At least below 70 cm depth, there were three profiles in our dataset with high observed SOC stocks (Figure 2). Those were not met by the predictions. The three profiles were polygenetic, one having a fossil Podzol profile below eolic sand deposits. The other two were classified as fluviatile soils. However, one profile had colluvial material on top, and the other was underlain by a fossil, carbonate-rich solifluctive soil. Although the impact of soil erosion and burial is not a particularly new challenge (Van Oost et al., 2005), there is currently no easy solution in spatial modelling to capture these effects.

The wide scatter of FFC predictions (Figure 2) can additionally be attributed to missing spatial information about the forest stand age and canopy structure (Bárcena et al., 2014; Böttcher and Springob, 2001; Penne et al., 2010), or detailed species composition (Rehschuh et al., 2021). Overall, total model and depth patterns performance are well within the upper range of reported studies. We attribute this to the inclusion of pedological knowledge in the model (Ma et al., 2019), but also to the detailed soil map of Hesse. Without spatial explicit information of soil properties, most of our covariates could not have been used for spatial modeling and upscaling from NFSI plots to forest sites of the federal state of Hesse.

We found that aggregated SOC stocks (*i.e.*, stocks of 0–90 cm of the mineral soil) had better validation measures as compared to individual depth increments. We suspect that this finding can be explained by inaccuracies of the modeled depth distribution. If modelled and observed depth gradients are shifted, the consequence is an overestimation at one layer and an underestimation in a neighboring layer. This shift in the depth distribution could be cancelled out, when aggregating OC stocks over several depth increments.

4.2 | Ecological relevance and sensitivity of covariates

In the following paragraphs, we discuss the sensitivity of individual covariates using standardized OC profiles. The standardized profiles, however, do not represent fully realistic conditions. For instance, we kept the proportion of coarse fragments constant with depth, which would realistically increase. Another example is the combination of soil classes and parent materials, which would not naturally occur. Therefore, the reader has to keep in mind that the standardized profiles serve the purpose to interpret the effect of a single covariate and not represent naturally occurring combinations of environmental conditions.

4.2.1 | Forest floor

Stocks of FFC under broadleaf forest were reported to be on average 44% of coniferous forest stocks (Peng et al., 2020). This finding fits very well with our results (Figure 4; 41% FFC stock under broadleaf, compared to coniferous forest). de Vos et al. (2015) showed that tree species affected FFC stocks markedly. This was also the case in the NFSI dataset (not shown; Grüneberg et al., 2019), but statewide spatial

coverage of tree species composition is incomplete and could thus not be used for regionalization.

Soil classes were grouped according to their effect sizes on FFC stocks. Colluvial soils and Chernozems were predicted to have the lowest FFC stocks. This can be explained due to high biotic activity in these soils (Persson and Wirén, 1993; Schaefer et al., 2009). Water-affected soil classes (Gley- and Stagnosols) showed the highest FFC stocks due to impeded decomposition by high moisture, and lower rooting depths (Chapin III et al., 2011). Strongly acidic conditions in Podzols also hamper decomposition and bioturbation (Persson and Wirén, 1993; Schaefer et al., 2009). The effect of acidity is also consistent with the predicted effects of the degree of podzolization.

Atmospheric nitrogen deposition is known to increase plant productivity, alter the amount and chemistry of litter, and often resulted in increased OC storage in vegetation and soils (de Vries et al., 2009; Etzold et al., 2020; Kwon et al., 2021). Several studies have shown that in N-poor ecosystems, the addition of N is likely to stimulate early-stage litter decomposition, whereas in N-sufficient ecosystems inhibitory effects have been reported through reduced activity of lignolytic fungi and a decreased exoenzymatic activity (Janssens et al., 2010). Mayer et al. (2020) reported that nitrogen addition consistently increased soil OC stocks across a wide range of forest ecosystems. Most studies (see de Vries et al., 2009) used fertilization experiments or isotopic tracers to deduct nitrogen-induced OC accumulation in soil, resulting in increases of 5 to 30 kg C $(kg\ N)^{-1}$. For example, Forsmark et al. (2020) reported a gradual increase in FFC stocks under Scots Pine by ca. 5, 6, 7, and 14 t ha^{-1} with additions of 3, 6, 12, and 50 kg N ha^{-1} y^{-1} for 13 years. In our study, the difference of FFC stocks between N deposition rates between 10 and 35 kg ha^{-1} y^{-1} was 22 t ha^{-1} in coniferous forests (Figure 4C). Although this is more than the reported 14 t ha^{-1} increase at higher deposition rate (Forsmark et al., 2020), the different time of exposure could account for this difference. Accumulation of FFC can also be mediated by acidification with increasing N deposition (Meesenburg et al., 2019; Meiwes et al., 2009; Persson and Wirén, 1993).

Since the NFSI was carried out over the course of 3 years, we accounted for sampling time. The seasonal dynamics of litterfall and decomposition were captured well by the model (Figure 4D). We choose the month of June for predictions, since FFC stocks in this month represent the average over the seasonal course.

The effect of climate differed between varying parent materials (Figure 4E,F). The general assumption is that decomposition of litter is hampered under cool, dry, and wet conditions, where FFC stocks are consequently high (Djukic et al., 2018). However, this pattern was confirmed mainly on the biome scale, when averaging litter decomposition across site conditions within a specific biome (Bradford et al., 2016; Djukic et al., 2018). At finer scales, specific site conditions modulate the accumulation of FFC stocks, and thresholds of a certain factor may override the effects of others (Prescott, 2010). Berg (2014) even postulated that the effect of climate is mostly indirect by its effect on litter quality. Parent material exerts a strong effect on nutrient availability (Heitkamp et al., 2020) and, thus, litter quality. Moreover, biogenic activity is also related to soil properties, strongly affected by parent material (Ponge et al., 2014). This explains the relatively uniform effect of climate in soils with acidic parent material (Figure 4), where other factors than climate dominate the limitation of decomposition. Manning et al. (2015), for example, reported that the effect of MAT on decomposition depended on the pH value. In soils with base rich parent material, the effect of climate is much more pronounced. Decomposition at intermediate conditions (*e.g.*, moderate moisture and temperature, nutrient-rich litter) is generally favored. With higher precipitation, oxygen will become a limiting factor, and at drier conditions, water availability hampers decomposition (Prescott, 2010), and also bioturbation (Schaefer et al., 2009).

4.2.2 | Mineral soil

The effect of MAT and MAP on SOC stocks was rather complex (Figure 5A,B). The general view is, that increasing temperature decreases and increasing precipitation increases SOC stocks (Jungkunst et al., 2021; Springob et al., 2001). Most likely, interactions of decomposition of OC and productivity of vegetation interact with the water balance. That is, both decomposition of OC and plant productivity is hampered either by dry or wet conditions, but at different thresholds (Chapin III et al., 2011; Zhao et al., 2016). This can result in highly non-linear behavior, which was often not captured by linear models (Yu et al., 2021). In our data, we see a decrease in SOC stocks at the lowest MAT and highest MAP, which is likely a consequence of decreasing plant productivity. The highest effect of temperature on SOC stocks was found at moderate amounts of MAP, which fits the findings of Guo et al. (2006). Of all covariates, the MAT-MAP combination was the only one, where the parametrization dataspace did not fully match with the dataspace of the prediction dataset (see polygons in Figure 5B). Within the climatic range of Hesse, plausible, albeit uncertain responses were predicted. This issue will be discussed in more detail together with spatial uncertainties. However, artifacts occurred for sites outside the climatic range of the parametrization and inside the range of Hesse, when increasing the smoothing parameter *k* from 5 to 8. This was the case despite of apparently better model performance within the climatic range of the parametrization dataset. It shows that predictions outside the calibration range have to be handled with extreme care.

The effect of CEC_{pot} on SOC stocks was very large. Since CEC_{pot} is calculated from texture, this is consistent with the relationship of SOC stocks or concentrations and the fine fraction (Arrouays et al., 2006; Burke et al., 1989; Hassink, 1997). Fine particles have high surface areas and stabilize SOC by diverse physicochemical mechanisms (von Lützow et al., 2006). However, there is a finite capacity of fine particles to interact with organic matter (Stewart et al., 2007). This was shown for carbon-rich topsoils under French forests (Chen et al., 2019). Moreover, the relationship of SOC with fine particles in forest topsoils was reported as weaker as compared to carbon-poor subsoils (Schleuß et al., 2014). This weakened relationship between texture (*i.e.*, the covariate CEC_{pot}) and SOC enrichment may also partly explain the relatively poor fit of our model for the upper depth increments (Figure 3D).

The reduction of SOC stocks by increasing volumes of coarse fragments coincided excellent with the equation of stock calculation (Figure 5D). The higher predicted SOC stocks, as would be expected from the pure dilution effect of volumetric coarse fraction, can be explained by two factors. First, plant productivity and consequently C input in soil may be reduced disproportionally. Plants adapt well to environmental conditions and gather nutrients and water from soil made inaccessible to sampling (Heisner et al., 2004). Therefore, there may a higher OC enrichment in the fine soil (< 2 mm) with high contents of coarse fragments. Second, sampling or measurement errors may be involved. High contents of coarse fragments occur frequently at lower parts of the soil profile. OC contents are small and may be close to the detection limit, which introduces uncertainty. Precise volume-based sampling is also hampered by the presence of coarse fragments (Throop et al., 2012).

Soil properties as indicated by soil classes induced the largest variation in the distribution of SOC across the soil profile (Figure 5E). This can be attributed to pedogenic processes, that is, transformation, accumulation, and translocation (Kögel-Knabner and Amelung, 2021). For example, Luvisols had the lowest stocks in the upper part of the profile (ca. 10–30 cm), where the eluvial E horizon is located. High SOC stocks between 20 and 40 cm and low stocks at the top mirror the presence of the eluvial horizon and OC rich B horizon in Podzols. Especially for the interpretation of the effects of the soil classes, it is important to keep in mind that the sensitivity analysis only examines selected conditions. For instance, Podzols showed the highest total (0–100 cm) SOC stocks, whereas Gleysols did not differ from other soil classes in total stocks. This is counterintuitive, since across Europe Gleysols often have very high SOC stocks, followed by Cambisols and Luvisols, whereas Podzols often have lower stocks (de Vos et al., 2015). The deviation of our study with respect to model sensitivity effects and field observations is explained by interaction with other covariates. For example, Podzols stock on sandy soils with low CEC_{pot}, whereas Gleysols often have intermediate CEC_{pot} and develop from fluviatile parent material.

We expected a gradual decrease of SOC at the top (location of the eluvial A horizon) and a gradual increase at intermediate depth (location of the illuvial B horizon) with an increasing degree of podzolization. This clear pattern was not apparent in our study (Figure 5F). The reason for this finding must remain speculative. We suspect that there is a complex interaction of biotic (plant growth, decomposition) and abiotic (transformation and translocation) processes, which cannot be explored in detail within our dataset.

Parent material had a more pronounced effect on total stocks as compared to the distribution within the soil profile (Figure 5G). Soils with fluviatile parent material showed higher SOC stocks, presumably due to high groundwater levels which impede decomposition, and also by containing allochthonous OC already present during sedimentation. Base rich and acidic parent material, however, also showed different depth distributions. Soils with acidic parent material showed higher SOC stocks at the top, compared to base rich material. This is most likely an effect of low abundance of saprophagous organisms (*Lumbricidae* and *Diplopoda*) in acidic soils. These organisms play a dominant role in the incorporation of organic matter from leaf litter into the mineral soil (Schaefer et al., 2009). Parent materials are also often associated with texture. This effect, however, should be captured by the CEC_{pot}. Therefore, the high SOC stocks predicted for eolic sand (at otherwise constant conditions) means that SOC stocks in eolic sands are higher than expected from their low CEC_{pot} (and other environmental conditions). Acidic conditions and edaphic moisture deficit are likely explaining this finding (Persson and Wirén, 1993), because both factors impede decomposition. Of course, also C input to soil is reduced by moisture deficit or acidity due to lower plant productivity. However, up to a certain threshold, plant productivity is less reduced than decomposition due to different adaption strategies at sub-optimal conditions. This is, for example, demonstrated by a higher reduction in microbial as compared to plant respiration with increasing moisture deficit (Zhao et al., 2016).

The forest type (broadleaf, mixed, and coniferous) affected the predictions only to a small extent (Figure 5H). Rehschuh et al. (2021) reported from a meta-analysis that mixed forests had on average 9% higher SOC stocks down to 50 cm mineral soil compared to monospecific beech stands. Summing up our data to 50 cm, we also found that SOC stocks of mixed compared to broadleaf forests were 10% higher. However, this small difference was compensated in the depth increments below 50 cm. Differences in total SOC stocks (0–100 cm) were not predicted (100.6% and 101.5% of SOC stocks in broadleaf, compared to mixed and coniferous, respectively). This fits the results of de Vos et al. (2015), who reported that forest stand type had a low importance in explaining variation in SOC stocks down to 100 cm. Our analysis did not confirm studies, which report higher SOC stocks under broadleaf forest as compared to coniferous forest (Grüneberg et al., 2019; Peng et al., 2020). Our dataset is a subset of that of Grüneberg et al. (2019), so this finding was surprising at first. However, Grüneberg et al. (2019) analyzed observed sampling data and the authors stated that specific site conditions, such as richer parent material under broadleaf forest, may contribute to their finding. In our sensitivity analysis, other factors than forest type were held constant. We conclude that interpretation of the effect of forest type on SOC stocks has to take into account that site conditions are often not well comparable (Schleuß et al., 2014).

4.3 | OC stocks of forest soils in Hesse

The predicted spatial average of total OC stocks (forest floor to 100 cm) of Hesse was between 78 and 92.5 t ha^{-1} (95% CI, Table 3). This is less than the median for German forest soils, which was estimated to 105 t ha^{-1} from data of the NFSI (forest floor to 90 cm, Grüneberg et al., 2019). Wellbrock et al. (2017) estimated total forest soil OC stocks for Germany (including soils with histic properties) to 1215 Mt. Therefore, forest soils of Hesse store 5.6–6.6% (67.6–80.1 Mt) of the total amount stored in German forest soils (Wellbrock et al., 2017), while having about 8% of the total forest area. Lower OC stocks of Hesse compared to Germany were attributed to relatively high contents of coarse fragments in the mostly hilly or mountainous terrain (Paar et al., 2016). Using the NFSI database, Paar et al. (2016) estimated the total OC stocks from the NFSI for Hesse's forest soils to 80 t ha^{-1} (forest floor

to 90 cm without soils with histic properties). This estimate from spatial representative sampling, which was a part of the parametrization data set, fits the predicted range well (Table 3). Due to the slightly lower sampling depth (90 *vs.* 100 cm) the estimate of Paar et al. (2016) is in the lower range of the predicted interval. Moreover, OC-rich soils on fluviatile parent material were underrepresented by the grid sampling in Hesse (Heitkamp et al., 2020), which may result in a slight underestimation of average OC stocks by the NFSI grid sampling. Organic soils store about 500 to 600 t OC ha^{-1}, but cover only 0.1% of Hesse's forest area. This results in a negligible addition of 0.4 to 0.5 Mt to the predicted total OC stock of Hesse of 67.6–80.1 Mt.

The proportion of 16% to 24% of OC stored in the forest floor in Hesse covers the values of 15–20% (NFSI Hesse, observation) and 18% (NFSI Germany) reported before (Grüneberg et al., 2019; Paar et al., 2016). Russ et al. (2021) reported a proportion of 30% of FFC for Brandenburg. The federal-state Brandenburg is characterized by high proportions of sandy, acidic soils and coniferous forest stands (Scots pine), which explains this finding. It is well proven that FFC stocks are generally higher under coniferous forests, as compared to mixed, or deciduous stands (de Vos et al., 2015). The aim to reduce the share of pure coniferous forests in Germany therefore leads to the expectation that parts of the FFC stocks will be lost in the future. From a purely carbon-accounting point of view, this seems counterproductive to the aim of carbon storage in forest ecosystems. However, it was shown that FFC is a much more labile pool than SOC in the mineral soil. FFC stocks react very sensitive to changing environmental conditions, such as management, tree species composition, climate, age of the forest stand, or litterfall (Brumme et al., 2021; de Vos et al., 2015; Jandl et al., 2007; Mayer et al., 2020). Forest floor material also serves as fuel and high stocks can induce or aggravate forest fires. Therefore, FFC stocks should not be seen as a reliable pool for carbon sequestration measures. Moreover, the most common coniferous forest species in Germany, Norway spruce, has been shown to be vulnerable against climatic extremes (storms, drought) and biotic calamities (Albert et al., 2018; Schuldt et al., 2020). It would seem grossly negligent to prevent development of resilient forests with the argument of less FFC storage.

The proportion of SOC stored in the topsoil (68–69% in 0–30 cm; Table 3) was predicted to be higher than the global average (approx. 50%; Jobbágy and Jackson, 2001), fits the proportion of NFSI observations (67%), and slightly lower than reported for terrestrial soils of Brandenburg (approx. 74%; Russ et al., 2021). Increasing SOC stocks in the subsoil is currently discussed as a mean to reduce the increase of atmospheric CO_2 concentrations (Whitmore et al., 2015), because SOC in subsoils generally has high mean residence times. The relatively low proportion of SOC in forest subsoils of Hesse may indicate that there is some potential for subsoil SOC storage. Although this potential should not be neglected, limitations of SOC storage should be clear (Powlson et al., 2011): (1) Additional OC storage in soil is finite, because after a certain amount of time a new dynamic equilibrium state will be reached; (2) increased amounts of SOC can also increase greenhouse gas emissions, especially N_2O; and (3) SOC storage is reversible, for example, by climatic or land use changes. Regarding recent climatic extremes with adverse effects on Central European forest ecosystems (Schuldt et al., 2020) it is important to increase the resilience of managed forests in order to maintain the ecosystem. Site-specific planning and diversification of planted forests are proposed to achieve this goal (Messier et al., 2021, and references therein). There are a few indications that tree diversity also increases SOC storage in a more stable form (Desie et al., 2019; Mayer et al., 2020; Schleuß et al., 2014). If true, this would be a win-win situation, which should be incentivized to forestry stakeholders.

4.4 | Spatial uncertainty

The highest uncertainties occurred independent of depth increment for forest soils at high elevation. The highest elevations are often characterized by soils with extreme properties, such as high content of coarse fragments, cool and wet climate, high N deposition, and otherwise rare soil classes. Three areas always associated with high uncertainty are the Hoher Meißner (North-East), the Rhön Mountains (East), and the Odenwald (South). The combination of MAT and MAP was outside the parametrization range (Figures 4 and 5). Rhön and Hoher Meißner had MAP around 1000 mm y^{-1} with MAT around 6°C, whereas especially lower locations of the Odenwald were characterized by high MAT (9–10°C) and high MAP (> 1000 mm y^{-1}). At the Vogelsberg (center) especially prediction of the FFC stocks was highly uncertain. Climatic data were within the parametrization range. However, N deposition was above 20 kg ha^{-1} y^{-1} and Stagnosols are predominant. Both covariates were associated with high uncertainties in the forest floor model (Figure 4). Mountains are often underrepresented in spatial sampling and predictions are therefore sometimes even omitted (*e.g.*, de Brogniez et al., 2015). Although locations at high elevations are not always of high spatial importance, they often store disproportional high amounts of OC (Hagedorn et al., 2010). Mountain soils are also highly affected by climate change (Rogora et al., 2018; Tito et al., 2020). Therefore, it will be important to adjust sampling strategies of inventories to better capture environmental conditions. Other areas of high uncertainty were characterized by colluvial soils, which cover 3.9% of Hesse's forest area, but only three profiles were in our database (0.8%). Non-histic Gleysols are represented better (11 profiles, 3.1% with 3.5% spatial coverage), but exhibit a high variability of OC stocks. Using spatial information about groundwater levels may have decreased uncertainty in this case (Russ et al., 2021).

In general, the uncertainty taken into account is solely the model uncertainty. Heuvelink (2018) lists other sources, such as uncertainty from attributes, position, or covariates. For example, uncertainties in temperature, precipitation, and nitrogen deposition estimates arise from various sources such as data, sampling, or regionalization errors. In addition, there are errors from the models used to estimate the total nitrogen deposition (Ahrends et al., 2020). Including these other sources of uncertainty will probably increase the general level of uncertainty in our study. However, estimating uncertainty from sampling, analytical errors, and generalization of spatial data is challenging (König et al., 2013). While our uncertainty assessment may be

incomplete, we are confident that the spatial pattern of total uncertainty will not change generally. Therefore, critical regions, where care has to be taken with interpretation of the predicted OC stocks, were identified in our study.

5 | CONCLUSIONS

With this study, we provide the first spatially explicit map for OC stocks in forest soils of Hesse at a scale of 1:50,000. The predicted OC stocks of the forest floor and the mineral soil in 5 cm depth increments can be calculated flexible to desired depths. The effect size and direction of the used covariates (*e.g.*, climate, forest type, parent material, texture, content of coarse fragments, N deposition, soil depth) are in a convincing range and comparable contexts, as reported by other studies. This raises confidence that our models fitted observations well for the right reasons, and is important in communication with forestry stakeholders, and for climate change mitigation reporting. Our predictions can be explained and communicated using common pedological knowledge. Uncertainty of the predictions is presented, which is crucial when using OC stocks as the base for dynamic prediction of stock changes with respect to climate change or forest management. The presented hierarchical model may well be used in other regions or states, and the results as a basis for dynamic carbon modeling for assessment of land-use and climate change effects on OC stocks in forest soils. However, sound knowledge of the spatial distribution of implemented covariates is prerequisite for the model application.

ACKNOWLEDGMENT

The work was funded by *Hessisches Ministerium für Umwelt, Klimaschutz, Landwirtschaft und Verbraucherschutz* (*Integrierter Klimaschutzplan Hessen 2025*, *Projekte L–12 & LF–06*). Open Access funding enabled and organized by Projekt DEAL.

DATA AVAILABILITY STATEMENT

The data that support the findings of this study are available from the corresponding author upon reasonable request.

ORCID

Felix Heitkamp https://orcid.org/0000-0002-0037-5553
Henning Meesenburg https://orcid.org/0000-0002-3035-4737

REFERENCES

Ad-hoc-Arbeitsgruppe Boden. (2005). *Bodenkundliche Kartieranleitung* (5th Ed.). Schweizerbart'sche Verlagsbuchhandlung.

Ahrends, B., Schmitz, A., Prescher, A. K., Wehberg, J., Geupel, M., Andreae, H., & Meesenburg, H. (2020). Comparison of methods for the estimation of total inorganic nitrogen deposition to forests in Germany. *Frontiers in Forests and Global Change*, *3*, 103. https://doi.org/10.3389/ffgc.2020.00103

Albert, M., Nagel, R. V., Nuske, R. S., Sutmöller, J., & Spellmann, H. (2017). Tree species selection in the face of drought risk—uncertainty in forest planning. *Forests*, *8*(10), 363. https://doi.org/10.3390/f8100363

Albert, M., Nagel, R. V., Sutmöller, J., & Schmidt, M. (2018). Quantifying the effect of persistent dryer climates on forest productivity and implications for forest planning: a case study in northern Germany. *Forest Ecosystems*, *5*(1), 1–21.

Angst, G., Mueller, K. E., Eissenstat, D. M., Trumbore, S., Freeman, K. H., Hobbie, S. E., Chorover, J., Oleksyn, J., Reich, P. B., & Mueller, C. W. (2019). Soil organic carbon stability in forests: distinct effects of tree species identity and traits. *Global change biology*, *25*(4), 1529–1546.

Arrouays, D., McBratney, A., Bouma, J., Libohova, Z., Richer-de-Forges, A. C., Morgan, C. L. S., Roudier, P., Poggio, L., & Mulder, V. L. (2020). Impressions of digital soil maps: The good, the not so good, and making them ever better. *Geoderma Regional*, *20*, e00255. https://doi.org/10.1016/j.geodrs.2020.e00255

Arrouays, D., Saby, N., Walter, C., Lemercier, B., & Schvartz, C. (2006). Relationships between particle-size distribution and organic carbon in French arable topsoils. *Soil Use and Management*, *22*(1), 48–51.

Bárcena, T. G., Kiær, L. P., Vesterdal, L., Stefánsdóttir, H. M., Gundersen, P., & Sigurdsson, B. D. (2014). Soil carbon stock change following afforestation in Northern Europe: a meta-analysis. *Global Change Biology*, *20*(8), 2393–2405.

Berg, B. (2014). Decomposition patterns for foliar litter–a theory for influencing factors. *Soil Biology and Biochemistry*, *78*, 222–232.

Bishop, T. F. A., McBratney, A. B., & Laslett, G. M. (1999). Modelling soil attribute depth functions with equal-area quadratic smoothing splines. *Geoderma*, *91*(1–2), 27–45.

Böttcher, J., & Springob, G. (2001). A carbon balance model for organic layers of acid forest soils. *Journal of Plant Nutrition and Soil Science*, *164*(4), 399–405.

Bradford, M. A., Berg, B., Maynard, D. S., Wieder, W. R., & Wood, S. A. (2016). Understanding the dominant controls on litter decomposition. *Journal of Ecology*, *104*(1), 229–238.

Brumme, R., Ahrends, B., Block, J., Schulz, C., Meesenburg, H., Klinck, U., Wagner, M., & Khanna, P. K. (2021). Cycling and retention of nitrogen in European beech (*Fagus sylvatica* L.) ecosystems under elevated fructification frequency. *Biogeosciences*, *18*(12), 3763–3779.

Bug, J., Heumann, S., Mueller, U., Waldeck, A. (2020). *Auswertungsmethoden im Bodenschutz - Dokumentation des Niedersächsichen Bodeninformationssystems (NIBIS)*. Landesamt für Bergbau, Energie und Geologie.

Burke, I. C., Yonker, C. M., Parton, W. J., Cole, C. V., Flach, K., & Schimel, D. S. (1989). Texture, climate, and cultivation effects on soil organic matter content in US grassland soils. *Soil Science Society of America Journal*, *53*(3), 800–805.

Camino-Serrano, M., Guenet, B., Luyssaert, S., Ciais, P., Bastrikov, V., De Vos, B., Gielen, B., Gleixner, G., Jornet-Puig, A., Kaiser, K., Kothawala, D., Lauerwald, R., Penuelas, J., Schrumpf, M., Vicca, S., Vuichard, N., Walmsley, D., & Janssens, I. (2018). ORCHIDEE-SOM: modeling soil organic carbon (SOC) and dissolved organic carbon (DOC) dynamics along vertical soil profiles in Europe. *Geoscientific Model Development*, *11*(3), 937–957.

Carey, C. J., Weverka, J., DiGaudio, R., Gardali, T., & Porzig, E. L. (2020). Exploring variability in rangeland soil organic carbon stocks across California (USA) using a voluntary monitoring network. *Geoderma Regional*, *22*, e00304. https://doi.org/10.1016/j.geodrs.2020.e00304

Chakan, A. A., Taghizadeh-Mehrjardi, R., Kerry, R., Kumar, S., Khordehbin, S., & Khanghah, S. Y. (2017). Spatial 3D distribution of soil organic carbon under different land use types. *Environmental monitoring and assessment*, *189*(3), 131. https://doi.org/10.1007/s10661–017–5830–9

Chapin III, F. S., Matson, P. A., & Vitousek, P. M. (2011). *Principles of terrestial ecosystem ecology* (2nd Ed.). Springer.

Chen, S., Arrouays, D., Angers, D. A., Martin, M. P., & Walter, C. (2019). Soil carbon stocks under different land uses and the applicability of the soil carbon saturation concept. *Soil and Tillage Research*, *188*, 53–58.

Cianfrani, C., Buri, A., Verrecchia, E., & Guisan, A. (2018). Generalizing soil properties in geographic space: Approaches used and ways forward. *PloS one*, *13*(12), e0208823. https://doi.org/10.1371/journal.pone.0208823

de Brogniez, D., Ballabio, C., Stevens, A., Jones, R. J. A., Montanarella, L., & van Wesemael, B. (2015). A map of the topsoil organic carbon content

of Europe generated by a generalized additive model. *European Journal of Soil Science*, *66*(1), 121–134.

de Vos, B., Cools, N., Ilvesniemi, H., Vesterdal, L., Vanguelova, E., & Carnicelli, S. (2015). Benchmark values for forest soil carbon stocks in Europe: Results from a large scale forest soil survey. *Geoderma*, *251*, 33–46.

de Vos, C., Don, A., Hobley, E. U., Prietz, R., Heidkamp, A., & Freibauer, A. (2019). Factors controlling the variation in organic carbon stocks in agricultural soils of Germany. *European Journal of Soil Science*, *70*(3), 550–564.

de Vos, C., Don, A., Prietz, R., Heidkamp, A., & Freibauer, A. (2016). Field-based soil-texture estimates could replace laboratory analysis. *Geoderma*, *267*, 215–219.

de Vries, W., Solberg, S., Dobbertin, M., Sterba, H., Laubhann, D., van Oijen, M., Evans, C., Gundersen, P., Kros, J., Wamelink, G. W. W., Reinds, G. J., & Sutton, M. A. (2009). The impact of nitrogen deposition on carbon sequestration by European forests and heathlands. *Forest Ecology and Management*, *258*(8), 1814–1823.

Desie, E., Vancampenhout, K., Heyens, K., Hlava, J., Verheyen, K., & Muys, B. (2019). Forest conversion to conifers induces a regime shift in soil process domain affecting carbon stability. *Soil Biology and Biochemistry*, *136*, 107540.

Djukic, I., Kepfer-Rojas, S., Schmidt, I. K., Larsen, K. S., Beier, C., Berg, B., Verheyen, K., Caliman, A., Paquette, A., Gutiérrez-Girón, A., Humber, A., Valdecantos, A., Petraglia, A., Alexander, H., Augustaitis, A., Saillard, A., Fernández, A. C. R., Sousa, A. I., Lillebø, A. I. … Tóth, Z. (2018). Early stage litter decomposition across biomes. *Science of the Total Environment*, *628*, 1369–1394.

Etzold, S., Ferretti, M., Reinds, G. J., Solberg, S., Gessler, A., Waldner, P., Schaub, M., Simpson, D., Benham, S., Hansen, K., Ingerslev, M., Jonard, M., Karlsson, P. E., Lindroos, A.-J., Marchetto, A., Manninger, M., Meesenburg, H., Merilä, P., Nöjd, P., … de Vries, W. (2020). Nitrogen deposition is the most important environmental driver of growth of pure, even-aged and managed European forests. *Forest Ecology and Management*, *458*, 117762. https://doi.org/10.1016/j.foreco.2019.117762

Evers, J., Damman, I., König, N., Paar, U., Stüber, V., Schulze, A., Schmidt, M., Schönfelder, E., & Eichhorn, J. (2019). *Waldbodenzustandsbericht für Niedersachsen und Bremen*. Ergebnisse der zweiten Bodenzustandserhebung im Wald (BZE II). Universitätsverlag Göttingen.

Fleck, S., Ahrends, B., Sutmöller, J., Albert, M., Evers, J., & Meesenburg, H. (2017). Is biomass accumulation in forests an option to prevent climate change induced increases in nitrate concentrations in the North German Lowland? *Forests*, *8*(6), 219. https://doi.org/10.3390/f8060219

Fleck, S., Cools, N., de Vos, B., Meesenburg, H., & Fischer, R. (2016). The Level II aggregated forest soil condition database links soil physicochemical and hydraulic properties with long-term observations of forest condition in Europe. *Annals of Forest Science*, *73*(4), 945–957.

Forsmark, B., Nordin, A., Maaroufi, N. I., Lundmark, T., & Gundale, M. J. (2020). Low and high nitrogen deposition rates in northern coniferous forests have different impacts on aboveground litter production, soil respiration, and soil carbon stocks. *Ecosystems*, 1–14.

Gomes, L. C., Faria, R. M., de Souza, E., Veloso, G. V., Schaefer, C. E. G., & Fernandes Filho, E. I. (2019). Modelling and mapping soil organic carbon stocks in Brazil. *Geoderma*, *340*, 337–350.

Grüneberg, E., Schöning, I., Riek, W., Ziche, D., & Evers, J. (2019). Carbon stocks and carbon stock changes in German forest soils. In N. Wellbrock & A. Bolte (Eds.), *Status and dynamics of forests in Germany: Results of the National Forest Monitoring* (pp. 167–198). Springer International Publishing.

Guckland, A., Ahrends, B., Paar, U., Dammann, I., Evers, J., Meiwes, K. J., Schönfelder, E., Ullrich, T., Mindrup, M., König, N., & Eichhorn, J. (2012). Predicting depth translocation of base cations after forest liming: results from long-term experiments. *European Journal of Forest Research*, *131*(6), 1869–1887.

Guo, Y., Gong, P., Amundson, R., & Yu, Q. (2006). Analysis of factors controlling soil carbon in the conterminous United States. *Soil Science Society of America Journal*, *70*(2), 601–612.

Hagedorn, F., Mulder, J., & Jandl, R. (2010). Mountain soils under a changing climate and land-use. *Biogeochemistry*, *97*(1), 1–5.

Hartemink, A. E., & Minasny, B. (2016). *Digital soil morphometrics* (1st Ed.). Springer.

Hassink, J. (1997). The capacity of soils to preserve organic C and N by their association with clay and silt particles. *Plant and Soil*, *191*(1), 77–87.

Heisner, U., Raber, B., & Hildebrand, E. E. (2004). The importance of the soil skeleton for plant-available nutrients in sites of the Southern Black Forest, Germany. *European Journal of Forest Research*, *123*(4), 249–257.

Heitkamp, F., Ahrends, B., Evers, J., Steinicke, C., & Meesenburg, H. (2020). Inference of forest soil nutrient regimes by integrating soil chemistry with fuzzy-logic: Regionwide application for stakeholders of Hesse, Germany. *Geoderma Regional*, *23*, e00340. https://doi.org/10.1016/j.geodrs.2020.e00340

Hengl, T., de Jesus, J. M., MacMillan, R. A., Batjes, N. H., Heuvelink, G. B. M., Ribeiro, E., Samuel-Rosa, A., Kempen, B., Leenaars, J. G. B., Walsh, M. G., & Gonzalez, M. R. (2014) SoilGrids1km—global soil information based on automated mapping. *PloS one*, *9*(8), e105992. https://doi.org/10.1371/journal.pone.0105992

Hengl, T., Kempen, B., Heuvelink, G., & Malone, B. (2019). Global Soil Information Facilities [R package GSIF version 0.5–5]. *Comprehensive R Archive Network (CRAN)*.

Hessisches Landesamt für Naturschutz, Umwelt und Geologie. (2018). *Erläuterung zu den Bodenflächendaten und zur Bodenkarte von Hessen 1:50 000* (2nd Ed.). Hessisches Landesamt für Naturschutz, Umwelt und Geologie.

Hessisches Ministerium für Umwelt, Klimaschutz, Landwirtschaft und Verbraucherschutz. (2015). *Wald- und Forstwirtschaft in Hessen 2011–2014*. Hessisches Ministerium für Umwelt, Klimaschutz, Landwirtschaft und Verbraucherschutz.

Heuvelink, G. B. M. (2018). Uncertainty. In Y. Yigini, G. F. Olmedo, S. Reiter, R. Baritz, K. Viatkin & R. Vargas, R. (Eds.), *Soil organic carbon mapping cookbook* (pp. 109–121). FAO.

Hübener, H., Bülow, K., Fooken, C., Früh, B., Hoffmann, P., Höpp, S., Keuler, K., Menz, C., Mohr, V., Radtke, K., Ramthun, H., Steger, C., Toussaint, F., Warrach-Sagi, K., & Woldt, M. (2017). *ReKliEs-De Ergebnisbericht*. World Data Center for Climate (WDCC) at DKRZ.

HVBG. (2018). Amtlich topografisch-kartografisches Informationssystem. HVBG.

IUSS Working Group WRB. (2015). World reference base for soil resources 204, update 2015 (No. 106). FAO.

Jandl, R., Lindner, M., Vesterdal, L., Bauwens, B., Baritz, R., Hagedorn, F., Johnson, D. W., Minkkinen, K., & Byrne, K. A. (2007). How strongly can forest management influence soil carbon sequestration? *Geoderma*, *137*(3–4), 253–268.

Jansen, V. M., Chodak, M., Saborowski, J., & Beese, E. (2005). Determination of humus stocks and qualities of forest floors in pure and mixed stands of spruce and beech. *Allgemeine Forst Und Jagdzeitung*, *176*(9–10), 176–186.

Janssens, I. A., Dieleman, W., Luyssaert, S., Subke, J.-A., Reichstein, M., Ceulemans, R., Ciais, P., Dolman, A. J., Grace, J., Matteucci, G., Papale, D., Piao, S. L., Schulze, E.-D., Tang, J., & Law, B. E. (2010). Reduction of forest soil respiration in response to nitrogen deposition. *Nature Geoscience*, *3*(5), 315–322.

Jenny, H. (1941). *Factors of soil formation: a system of quantitative pedology*. McGraw-Hill.

Jobbagy, E. G., & Jackson, R. B. (2001). The distribution of soil nutrients with depth: global patterns and the imprint of plants. *Biogeochemistry*, *53*(1), 51–77.

Jungkunst, H. F., Goepel, J., Horvath, T., Ott, S., & Brunn, M. (2021). New uses for old tools: Reviving Holdridge Life Zones in soil carbon persistence research. *Journal of Plant Nutrition and Soil Science*, *184*(1), 5–11.

Kempen, B., Brus, D. J., & Heuvelink, G. B. M. (2018). Validation. In Y. Yigini, G. F. Olmedo, S. Reiter, R. Baritz, K. Viatkin & R. Vargas, R. (Eds.), *Soil organic carbon mapping cookbook* (pp. 122–140). FAO.

Kögel-Knabner, I., & Amelung, W. (2021). Soil organic matter in major pedogenic soil groups. *Geoderma*, *384*, 114785. https://doi.org/10.1016/j.geoderma.2020.114785

König, N., Cools, N., Derome, K., Kowalska, A., de Vos, B., Fürst, A., Marchetto, A., O'Dea, P., & Tartari, G. A. (2013). Data quality in laboratories: Methods and results for soil, foliar, and water chemical analyses. In M. Ferretti & R. Fischer (Eds.), *Developments in Environmental Science* (pp. 415–453). Elsevier.

Kravchenko, A. N., & Robertson, G. P. (2011). Whole-profile soil carbon stocks: The danger of assuming too much from analyses of too little. *Soil Science Society of America Journal*, *75*(1), 235–240.

Kwon, T., Shibata, H., Kepfer-Rojas, S., Schmidt, I. K., Larsen, K. S., Beier, C., Berg, B., Verheyen, K., Lamarque, J. - F., Hagedorn, F., Eisenhauer, N., Djukic, I., & TeaComposition Network. (2021). Effects of climate and atmospheric nitrogen deposition on early to mid-term stage litter decomposition across biomes. *Frontiers in Forests and Global Change*, 90. https://doi.org/10.3389/ffgc.2021.678480

Lal, R. (2005). Forest soils and carbon sequestration. *Forest Ecology and Management*, *220*(1–3), 242–258.

Lamichhane, S., Kumar, L., & Wilson, B. (2019). Digital soil mapping algorithms and covariates for soil organic carbon mapping and their implications: A review. *Geoderma*, *352*, 395–413.

Li, J. (2017). Assessing the accuracy of predictive models for numerical data: Not r nor r2, why not? Then what? *PloS One*, *12*(8), e0183250. https://doi.org/10.1371/journal.pone.0183250

Ma, Y., Minasny, B., Malone, B. P., & Mcbratney, A. B. (2019). Pedology and digital soil mapping (DSM). *European Journal of Soil Science*, *70*(2), 216–235.

Ma, Y., Minasny, B., McBratney, A., Poggio, L., & Fajardo, M. (2021). Predicting soil properties in 3D: Should depth be a covariate? *Geoderma*, *383*, 114794.

Malone, B. P., McBratney, A. B., Minasny, B., & Laslett, G. M. (2009). Mapping continuous depth functions of soil carbon storage and available water capacity. *Geoderma*, *154*(1–2), 138–152.

Manning, P., de Vries, F. T., Tallowin, J. R. B., Smith, R., Mortimer, S. R., Pilgrim, E. S., Harrison, K. A., Wright, D. G., Quirk, H., Benson, J., Shipley, B., Cornelissen, J. H. C., Kattge, J., Bönisch, G., Wirth, C., & Bardgett, R. D. (2015). Simple measures of climate, soil properties and plant traits predict national-scale grassland soil carbon stocks. *Journal of Applied Ecology*, *52*(5), 1188–1196.

Mayer, M., Prescott, C. E., Abaker, W. E. A., Augusto, L., Cécillon, L., Ferreira, G. W. D., James, J., Jandl, R., Katzensteiner, K., Laclau, J.-P., Laganière, J., Nouvellon, Y., Paré, D., Stanturf, J. A., Vanguelova, E. I., & Vesterdal, L. (2020). Tamm Review: Influence of forest management activities on soil organic carbon stocks: A knowledge synthesis. *Forest Ecology and Management*, *466*, 118127. https://doi.org/10.1016/j.foreco.2020.118127

McBratney, A. B., Santos, M. M., & Minasny, B. (2003). On digital soil mapping. *Geoderma*, *117*(1–2), 3–52.

Meesenburg, H., Riek, W., Ahrends, B., Eickenscheidt, N., Grüneberg, E., Evers, J., Fortmann, H., König, N., Lauer, A., Meiwes, K. J., Nagel, H.-D., Schimming, C.-G., & Wellbrock, N. (2019). Soil acidification in German forest soils. In N. Wellbrock & A. Bolte, A. (Eds.), *Status and dynamics of forests in Germany: Results of the National Forest Monitoring* (pp. 93–121). Springer International Publishing.

Meiwes, K. J., Meesenburg, H., Eichhorn, J., Jacobsen, C., & Khanna, P. K. (2009): Changes in C and N Contents of soils under beech forests over a period of 35 years. In R. Brumme & P. K. Khanna (Eds.), *Functioning and management of European beech ecosystems* (pp. 49–63). Springer.

Messier, C., Bauhus, J., Sousa-Silva, R., Auge, H., Baeten, L., Barsoum, N., Bruelheide, H., Caldwell, B., Cavender-Bares, J., Dhiedt, E., Eisenhauer, N., Ganade, G., Gravel, D., Guillemot, J., Hall, J. S., Hector, A., Hérault, B., Jactel, H., Koricheva, J., … Zemp, D. C. (2021). For the sake of resilience and multifunctionality, let's diversify planted forests! *Conservation Letters*, e12829. https://doi.org/10.1111/conl.12829

Mulder, V. L., Lacoste, M., Richer-de-Forges, A. C., Martin, M. P., & Arrouays, D. (2016). National versus global modelling the 3D distribution of soil organic carbon in mainland France. *Geoderma*, *263*, 16–34.

Nauman, T. W., & Duniway, M. C. (2019). Relative prediction intervals reveal larger uncertainty in 3D approaches to predictive digital soil mapping of soil properties with legacy data. *Geoderma*, *347*, 170–184.

Nussbaum, M., Papritz, A., Baltensweiler, A., & Walthert, L. (2014). Estimating soil organic carbon stocks of Swiss forest soils by robust external-drift kriging. *Geoscientific Model Development*, *7*(3), 1197–1210.

Paar, U., Evers, J., Damman, I., König, N., Schulze, A., Schmidt, M., Schönfelder, E., Scheler, B., Ullrich, T., & Eichhorn, J. (2016). *Waldbodenzustandsbericht für Hessen. Ergebnisse der zweiten Bodenzustandserhebung im Wald (BZE II)*. Universitätsverlag Göttingen.

Panferov, O., Doering, C., Rauch, E., Sogachev, A., & Ahrends, B. (2009). Feedbacks of windthrow for Norway spruce and Scots pine stands under changing climate. *Environmental Research Letters*, *4*(4), 045019. https://doi.org/10.1088/1748–9326/4/4/045019

Paul, C., Brandl, S., Friedrich, S., Falk, W., Härtl, F., & Knoke, T. (2019). Climate change and mixed forests: how do altered survival probabilities impact economically desirable species proportions of Norway spruce and European beech? *Annals of Forest Science*, *76*(1), 1–15.

Pedersen, E. J., Miller, D. L., Simpson, G. L., & Ross, N. (2019). Hierarchical generalized additive models in ecology: an introduction with mgcv. *PeerJ*, *7*, e6876. https://doi.org/10.7717/peerj.6876

Peng, Y., Schmidt, I. K., Zheng, H., Hedĕnec, P., Bachega, L. R., Yue, K., Wu, F., & Vesterdal, L. (2020). Tree species effects on topsoil carbon stock and concentration are mediated by tree species type, mycorrhizal association, and N-fixing ability at the global scale. *Forest Ecology and Management*, *478*, 118510. https://doi.org/10.1016/j.foreco.2020.118510

Penne, C., Ahrends, B., Deurer, M., & Böttcher, J. (2010). The impact of the canopy structure on the spatial variability in forest floor carbon stocks. *Geoderma*, *158*(3–4), 282–297.

Persson, T., & Wirén, A. (1993). Effects of experimental acidification on C and N mineralization in forest soils. *Agriculture, Ecosystems & Environment*, *47*(2), 159–174.

Piñeiro, G., Perelman, S., Guerschman, J. P., & Paruelo, J. M. (2008). How to evaluate models: observed *vs.* predicted or predicted *vs.* observed? *Ecological Modelling*, *216*(3–4), 316–322.

Poeplau, C., Jacobs, A., Don, A., Vos, C., Schneider, F., Wittnebel, M., Tiemeyer, B., Heidkamp, A., Prietz, R., & Flessa, H. (2020). Stocks of organic carbon in German agricultural soils—Key results of the first comprehensive inventory. *Journal of Plant Nutrition and Soil Science*, *183*(6), 665–681.

Ponge, J. F., Sartori, G., Garlato, A., Ungaro, F., Zanella, A., Jabiol, B., & Obber, S. (2014). The impact of parent material, climate, soil type and vegetation on Venetian forest humus forms: A direct gradient approach. *Geoderma*, *226*, 290–299.

Powlson, D. S., Whitmore, A. P., & Goulding, K. W. (2011). Soil carbon sequestration to mitigate climate change: a critical re-examination to identify the true and the false. *European Journal of Soil Science*, *62*(1), 42–55.

Prescott, C. E. (2010). Litter decomposition: what controls it and how can we alter it to sequester more carbon in forest soils? *Biogeochemistry*, *101*(1), 133–149.

R Core Team. (2017). *R: A language and environment for statistical computing*. R Foundation for Statistical Computing.

Rehschuh, S., Jonard, M., Wiesmeier, M., Rennenberg, H., & Dannenmann, M. (2021). Impact of European beech forest diversification on soil organic carbon and total nitrogen stocks–a meta-analysis. *Frontiers in Forests and Global Change*, *4*, 606669. https://doi.org/10.5445/IR/1000133854

Richter, D. D., & Yaalon, D. H. (2012). "The changing model of soil" revisited. *Soil Science Society of America Journal*, *76*(3), 766–778.

Rogora, M., Frate, L., Carranza, M., Freppaz, M., Stanisci, A., Bertani, I., Bottarin, R., Brambilla, A., Canullo, R., Carbognani, M., Cerrato, C., Chelli, S., Cremonese, E., Cutini, M., Di Musciano, M., Erschbamer, B., Godone,

D., Iocchi, M., Isabellon, M., & Matteucci, G. (2018). Assessment of climate change effects on mountain ecosystems through a cross-site analysis in the Alps and Apennines. *Science of the total environment*, *624*, 1429–1442.

Russ, A., Riek, W., & Wessolek, G. (2021). Three-dimensional mapping of forest soil carbon stocks using SCORPAN modelling and relative depth gradients in the North-Eastern lowlands of Germany. *Applied Sciences*, *11*(2), 714. https://doi.org/10.3390/app11020714

Schaap, M., Wichink Kruit, R. J., Kranenburg, R., Segers, A., Builtjes, P., Banzhaf, S., & Scheuschner, T. (2015). Atmospheric deposition to German natural and semi-natural ecosystems during 2009. *Project No.(FKZ)*, *3712*(63), 240–1. Umweltbundesamt.

Schaefer, M., Migge-Kleian, S., Scheu, S. (2009). The role of soil fauna for decomposition of plant residues. In R. Brumme & P. K. Khanna (Eds.), *Functioning and management of European beech ecosystems* (pp. 207–230). Springer.

Schleuß, P. M., Heitkamp, F., Leuschner, C., Fender, A. C., & Jungkunst, H. F. (2014). Higher subsoil carbon storage in species-rich than species-poor temperate forests. *Environmental Research Letters*, *9*(1), 014007. https://doi.org/10.1088/1748–9326/9/1/014007

Schrumpf, M., Schulze, E. D., Kaiser, K., & Schumacher, J. (2011). How accurately can soil organic carbon stocks and stock changes be quantified by soil inventories? *Biogeosciences*, *8*(5), 1193–1212.

Schuldt, B., Buras, A., Arend, M., Vitasse, Y., Beierkuhnlein, C., Damm, A., Gharun, M., Grams, T. E. E., Hauck, M., Hajek, P., Hartmann, H., Hiltbrunner, E., Hoch, G., Holloway-Phillips, M., Körner, C., Larysch, E., Lübbe, T., Nelson, D. B., Rammig, A., … Kahmen, A. (2020). A first assessment of the impact of the extreme 2018 summer drought on Central European forests. *Basic and Applied Ecology*, *45*, 86–103.

Soucémarianadin, L. N., Cécillon, L., Guenet, B., Chenu, C., Baudin, F., Nicolas, M., Girardin, C., & Barré, P. (2018). Environmental factors controlling soil organic carbon stability in French forest soils. *Plant and Soil*, *426*(1), 267–286.

Springob, G., Brinkmann, S., Engel, N., Kirchmann, H., & Böttcher, J. (2001). Organic C levels of Ap horizons in North German Pleistocene sands as influenced by climate, texture, and history of land-use. *Journal of Plant Nutrition and Soil Science*, *164*(6), 681–690.

Stewart, C. E., Paustian, K., Conant, R. T., Plante, A. F., & Six, J. (2007). Soil carbon saturation: concept, evidence and evaluation. *Biogeochemistry*, *86*(1), 19–31.

Temperli, C., Bugmann, H., & Elkin, C. (2012). Adaptive management for competing forest goods and services under climate change. *Ecological Applications*, *22*(8), 2065–2077.

Thiele, J. C., Nuske, R. S., Ahrends, B., Panferov, O., Albert, M., Staupendahl, K., Junghans, U., Jansen, M., & Saborowski, J. (2017). Climate change impact assessment—A simulation experiment with Norway spruce for a forest district in Central Europe. *Ecological Modelling*, *346*, 30–47.

Throop, H. L., Archer, S. R., Monger, H. C., & Waltman, S. (2012). When bulk density methods matter: Implications for estimating soil organic carbon pools in rocky soils. *Journal of Arid Environments*, *77*, 66–71.

Tito, R., Vasconcelos, H. L., & Feeley, K. J. (2020). Mountain ecosystems as natural laboratories for climate change experiments. *Frontiers in Forests and Global Change*, *3*, 38. https://doi.org/10.3389/ffgc.2020.00038

Van Oost, K., Govers, G., Quine, T. A., Heckrath, G., Olesen, J. E., De Gryze, S., & Merckx, R. (2005). Landscape-scale modeling of carbon cycling under the impact of soil redistribution: The role of tillage erosion. *Global Biogeochemical Cycles*, *19*(4). https://doi.org/10.1029/2005GB002471

Vereecken, H., Schnepf, A., Hopmans, J. W., Javaux, M., Or, D., Roose, T., Vanderborght, J., Young, M. H., Amelung, W., Aitkenhead, M., Allison, S. D., Assouline, S., Baveye, P., Berli, M., Brüggemann, N., Finke, P., Flury, M., Gaiser, T., Govers, G., … Young, I. M. (2016). Modeling soil processes: Review, key challenges, and new perspectives. *Vadose Zone Journal*, *15*(5). https://doi.org/10.2136/vzj2015.09.0131

von Lützow, M. V., Kögel-Knabner, I., Ekschmitt, K., Matzner, E., Guggenberger, G., Marschner, B., & Flessa, H. (2006). Stabilization of organic matter in temperate soils: mechanisms and their relevance under different soil conditions–a review. *European Journal of Soil Science*, *57*(4), 426–445.

Webster, R., & Oliver, M. A. (2007). *Geostatistics for environmental scientists* (2nd Ed.). John Wiley & Sons.

Wellbrock, N., Ahrends, B., Bögelein, R., Bolte, A., Eickenscheidt, N., Grüneberg, E., König, N., Schmitz, A., Fleck, S., & Ziche, D. (2019): Concept and methodology of the National Forest Soil Inventory. In N. Wellbrock & A. Bolte (Eds.), *Status and dynamics of forests in Germany. Results of the National Forest Monitoring* (pp. 1–28). Springer Open.

Wellbrock, N., Grüneberg, E., Riedel, T., & Polley, H. (2017). Carbon stocks in tree biomass and soils of German forests. *Lesnicky Casopis*, *63*(2–3), 105–112.

Whitmore, A. P., Kirk, G. J. D., & Rawlins, B. G. (2015). Technologies for increasing carbon storage in soil to mitigate climate change. *Soil Use and Management*, *31*, 62–71.

Wood, S. N. (2017). *Generalized additive models: an introduction with R*. CRC Press.

Wood, S. (2019). Mixed GAM computation vehicle with automatic smoothness estimation. R package version 1. 8–12. Available at: https://cran.r-project.org/web/packages/mgcv/

Yang, R. - M., Zhang, G. - L., Yang, F., Zhi, J. - J., Yang, F., Liu, F., Zhao, Y. - G., & Li, D. C. (2016). Precise estimation of soil organic carbon stocks in the northeast Tibetan Plateau. *Scientific Reports*, *6*(1), 1–10.

Yu, W., Weintraub, S. R., & Hall, S. J. (2021). Climatic and geochemical controls on soil carbon at the continental scale: interactions and thresholds. *Global Biogeochemical Cycles*, *35*(3), e2020GB006781. https://doi.org/10.1029/2020GB006781

Zhao, C., Miao, Y., Yu, C., Zhu, L., Wang, F., Jiang, L., Hui, D., & Wan, S. (2016). Soil microbial community composition and respiration along an experimental precipitation gradient in a semiarid steppe. *Scientific Reports*, *6*(1), 1–9.

Ziche, D., Grüneberg, E., Hilbrig, L., Höhle, J., Kompa, T., Liski, J., Repo, A., & Wellbrock, N. (2019). Comparing soil inventory with modelling: Carbon balance in central European forest soils varies among forest types. *Science of the Total Environment*, *647*, 1573–1585.

How to cite this article: Heitkamp, F., Ahrends, B., Evers, J., & Meesenburg, H. (2021). Spatial 3D mapping of forest soil carbon stocks in Hesse, Germany. *Journal of Plant Nutrition and Soil Science*, 1–22. https://doi.org/10.1002/jpln.202100138